



Chemical characterization and synergetic source apportionment of PM_{2.5} at multiple sites in the Beijing-Tianjin-Hebei region, China

Xiaojuan Huang^{1,2}, Zirui Liu^{1,3*}, Jingyun Liu¹, Bo Hu¹, Tianxue Wen¹, Guiqian Tang¹,
Junke Zhang¹, Fangkun Wu¹, Dongsheng Ji¹, Lili Wang¹, Yuesi Wang^{1,3*}

5 ¹State Key Laboratory of Atmospheric Boundary Layer Physics and Atmospheric Chemistry (LAPC), Institute of
Atmospheric Physics, Chinese Academy of Sciences, Beijing, China

²Plateau Atmosphere and Environment Key Laboratory of Sichuan Province, College of Atmospheric Sciences,
Chengdu University of Information Technology, Chengdu, China

10 ³Center for Excellence in Regional Atmospheric Environment, Institute of Urban Environment, Chinese Academy
of Sciences, Xiamen, China

*Corresponding author: Zirui Liu (liuzirui@mail.iap.ac.cn); Yuesi Wang (wys@mail.iap.ac.cn)

ABSTRACT: High frequencies of haze in China, especially in the Beijing-Tianjin-Hebei region,
have received widespread attention in recent years. In this study, samples of filtered atmospheric
15 fine particulate matter (PM_{2.5}) were collected synchronously at three urban sites (Beijing, Tianjin,
and Shijiazhuang) and at a regional background site (Xinglong) for one month during each season
from June 2014 to April 2015. Chemical composition determination/analysis, chemical mass
closure, positive matrix factorization (PMF) and backward trajectory clustering were employed to
investigate the chemical speciation, haze formation mechanism, emission sources, and influences
20 of regional transport in North China. Our results reported that the aerosol chemical compositions
were very similar at the urban sites and the background site and mainly comprised organic matter
(16.0%-25.0%), sulfate (14.4%-20.5%), nitrate (15.1%-19.5%), ammonium (11.6%-13.1%) and
mineral dust (14.7%-20.8%). Sources apportionment of PM_{2.5} by PMF model revealed that
25 secondary aerosols (background) and secondary inorganic aerosols (urban) were the dominant
sources, which accounted for 29.2%-45.1% of PM_{2.5} throughout the entire study and played a vital
role in the formation and development of haze pollution. Emissions of motor vehicle exhaust
exerted a significant impact on haze formation at urban sites, particularly at Beijing; and coal
combustion also played a dominant role in winter, especially at Shijiazhuang. Backward
trajectory analysis revealed that haze pollution has remarkable regional characteristics and usually
30 occurs when air masses originated from polluted industrial regions of the south prevailed, which
accompanied by high PM_{2.5} loadings with high contributions of secondary aerosols. This study
suggests that the control strategies to mitigate the haze formation in BTH region should be focused
on the emission reduction of gaseous precursors from fossil fuel combustion, particularly from
motor vehicles by improving the quality of oil products.

35 1 Introduction

Due to rapid economic development, rapid urbanization processes and excessive energy



consumption, regional haze pollution has been recognized as the most severe environmental problem in China and has received the extensive attention of the government, public and scientists in recent years (Zhang et al., 2015b). Haze pollution mainly occurs in economically developed urban agglomeration; the most seriously polluted regions are typically the Beijing-Tianjin-Hebei (BTH) region, the Yangtze River Delta (YRD) region, the Pearl River Delta region (PRD) and the Sichuan Basin (Zhang et al., 2012; Zhang and Cao, 2015). The BTH region, which includes the two megacities of Beijing and Tianjin as well as Hebei Province, has the highest density of coal consumption and heavily polluting industries in China and is surrounded by Shandong, Henan, Shanxi and Inner Mongolia, which are all heavily populated, industrialized, urbanized and frequently reported to have serious haze pollution due to their intensive emissions of air pollutants across China (Liang et al., 2016; Wang et al., 2014a). Therefore, because the BTH region features the strongest pollutant emissions (Zhao et al., 2012), unfavorable meteorological conditions (Cai et al., 2017; Xu et al., 2011), and its unique topography, extreme haze pollution, characterized by high particulate matter (PM) loading and very low visibility, has frequently occurred in this region. From 2014-2015, among the 190 priority pollution monitoring cities in China, the annual average concentration of atmospheric fine particulate matter (PM_{2.5}) was highest in the BTH region (Zhang and Cao, 2015). Additionally, this region is characterized by frequent dust storms and corresponding high mineral dust load episodes, especially in spring (Huang et al., 2010; Sun et al., 2010).

In addition to its the impacts on ecosystems, regional-scale atmospheric visibility, traffic safety, the economy, and interactions with climate (Zhang et al., 2015b), more importantly, such serious air pollution can have adverse effects on human health, including the increased risk of respiratory, cardiac and other medical conditions (Elliot et al., 2016; Wu et al., 2017), thus leading to increased mortality, especially in megacities, which are generally seriously polluted and densely populated. The health effects of PM are closely related to its chemical composition, in addition to the particle mass concentration and particle size (Zhang et al., 2015b). Tang et al. (2017) investigated the relationship between mortality and air pollution in Beijing from 1949 to 2011 and determined that the mortality in Beijing due to circulatory diseases was correlated with sulfate, nitrate and formaldehyde, whereas respiratory diseases were correlated with calcium, sulfate and nitrate, and malignant tumors were correlated with ammonium, nitrate and formaldehyde with an 11-year lag. In addition to their health impacts, the climate and environmental domino effects caused by PM are also closely related to the chemical compositions of PM, as have been widely reported (Tao et al., 2014; Wang et al., 2015b; Wu et al., 2009). These chemical constituents mainly originate from various anthropogenic sources, such as coal combustion, vehicle exhaust emissions, biomass burning, cooking, and industry-related emission, among others. Therefore, the key to reducing PM_{2.5} concentrations and improving air quality is to control these sources; this necessitates a strong demand for good knowledge about the detailed chemical compositions of



PM_{2.5} in the BTH region.

Haze pollution has significantly regional characteristics. In addition to local emissions, the regional or inter-regional transport of primary PM and gaseous precursors plays an important role during haze periods (Chen et al., 2017; Li et al., 2017, 2015; Tao et al., 2012; Wang et al., 2014a; 5 Ying et al., 2014). For example, the SO₂ measured in Beijing includes a large regional contribution transported from southern industrial areas (Guo et al., 2014). Therefore, these point to an urgent demand for wider collaborative work on emission control strategies with neighboring cities or provinces. For Shanghai, which is a megacity in the YRD region, Wu et al. (2017) estimated that the application of multiregional integrated control strategies in neighboring provinces could be 10 most effective in reducing PM_{2.5} in Shanghai and could largely reduce the economic loss caused by haze pollution. Haze pollution studies performed in the BTH region have obtained fruitful and meaningful results (Du et al., 2014; Liu et al., 2016a; Sun et al., 2013; Wang et al., 2014b; Zhang et al., 2014; Zhao et al., 2013c). The haze pollution in this region is primarily affected by low boundary layer height, southerly transport of water vapor and pollutants, and strong local 15 emissions (Tang et al., 2015a; Zhu et al., 2016). Regional civil/industrial energy consumption and urban transportation are the main sources of atmospheric pollutants (Guo et al., 2014; Zhao et al., 2012). Compared to primary particles, secondary species that are transformed by gaseous precursors, including secondary inorganic aerosols (SIA) and secondary organic aerosols (SOA), play a more important role in the haze formation (Huang et al., 2014; Sun et al., 2012; Wang et al., 20 2013b; Zhang et al., 2014). Particularly under high relative humidity, aqueous chemistry process could be largely promoted and results in efficient secondary formation (Hu et al., 2016). Moreover, recent studies have reported that a new efficient formation mechanism of sulfate, that is the aqueous oxidation of SO₂ by NO₂ under the conditions of relative high humidity during haze events (Cheng et al., 2016; He et al., 2014; Wang et al., 2016a, 2013b). On the issue of haze 25 mitigation strategies in Beijing, reducing regional emissions during the transition period and reducing local emissions during the polluted period was suggested (Tang et al., 2015a). However, because the studies describing the chemical composition and sources of PM_{2.5} in the BTH region were often conducted at single site or for short periods, long-term and multisite studies are scarce (Li et al., 2017; Shen et al., 2016; Tian et al., 2016; Zhang et al., 2013; Zong et al., 2016). 30 Single-site source apportionment data are not suitable for the comparing the results of different studies that used different methods of source analysis and data processing. Furthermore, studies of the source apportionment of PM_{2.5} usually reflect the average condition for a given period, whereas the evolution of emission sources under different pollution levels has barely been investigated. Therefore, these studies yield a narrow view of their temporal and spatial 35 characteristics and are not conducive to better understanding the mechanism of regional haze formation (Bressi et al., 2013).

To fill this gap, in this study, we conducted synchronous measurements of PM_{2.5} at three



urban sites (Beijing, Tianjin, Shijiazhuang) in the BTH region and at one regional background site (Xinglong), analyzed their chemical compositions and quantified the apportionment of their sources using unified data processing and analytical methods. In addition, we emphatically analyzed the the chemical compositions and emission sources at different pollution levels and their differences between sites, as well as the influence of air masses originating from different directions. This study could provide an overall understanding of the regional signal of PM_{2.5} pollution in the BTH region and support stakeholders and policy makers in understanding the impact of regional sources on the high loading of PM_{2.5}, thus facilitating the design of effective joint emission abatement strategies.

2. Materials and methods

2.1 Sites, sampling and meteorological data

Four sampling sites were selected in the Beijing-Tianjin-Hebei region (Fig. 1), including three urban sites (Beijing, Tianjin and Shijiazhuang) and a regional background site (Xinglong). These sites reflect the atmospheric pollutions condition in this region. The sampling site in Xinglong (117.58 E, 40.39 N) was located at Xinglong Observatory, National Astronomical Observatory, Chinese Academy of Sciences. Xinglong Observatory is located in the northeastern region of Beijing, which is located at a liner distance of approximately 110 km from Beijing and is surrounded by mountains and thus minimally affected by human activities. Therefore, it is one of the regional atmospheric background stations of the Chinese Academy of Sciences. The Beijing site (39.97 N, 116.38 E) was situated in the courtyard of the Institute of Atmospheric Physics (IAP), Chinese Academy of Sciences (CAS). The Tianjin site (39.09 E, 117.19 N) was located in the Tianjin Atmospheric Boundary Layer Observatory, Chinese Meteorological Administration, and the Shijiazhuang site (38.03 N, 114.53 E) was located in the Hebei Meteorological Service.

Meteorological data including ambient temperature, relative humidity and wind speed in Beijing were measured approximately 20 m to the filter sampling site, using an automatic meteorological observation instrument (Milos520, Vaisala, Finland), located at the 8 m measurement height. And in Tianjin, Shijiazhuang and Xinglong, the meteorological data was obtained from China Meteorological Administration.

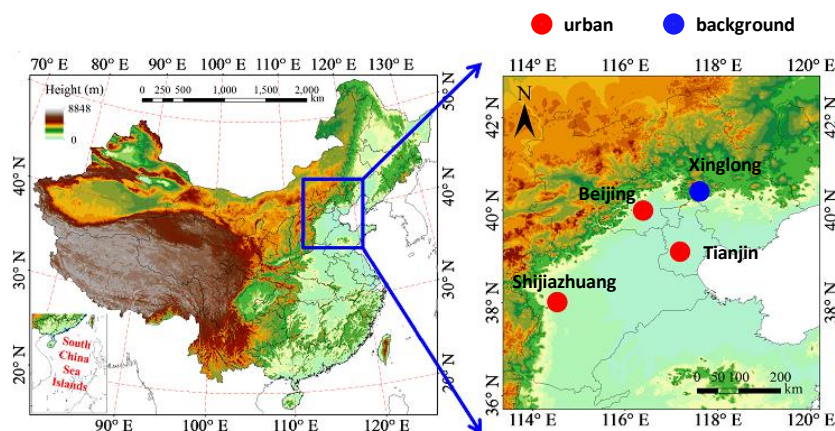


Figure 1. Map of the sampling sites (Beijing, Tianjin and Shijiazhuang are representatives of urban stations, whereas Xinglong represents the regional background)

5 $PM_{2.5}$ (particles with aerodynamic diameters of less than $2.5 \mu m$) samples were synchronously collected at the four sites using a $PM_{2.5}$ sampler (TH-150C, Tianhong, Wuhan) from June 2014 to April 2015. During each season, we collected $PM_{2.5}$ samples on quartz membrane filters every day and night for one month, except on rainy days. The specific sampling period for summer extended from 15 June 2014 to 14 July 2014, that of autumn extended from 15 September 2014 to 14 October 2014, that of winter extended from 29 December 2014 to 27 January 2015, and that of
10 spring extended from 20 March 2015 to 18 April 2015. The sampling time of each sample was 11.5 h, which generally occurred from 8:00 am to 19:30 pm during the daytime and from 20:00 pm to 7:30 am of the next day during the nighttime. During the entire observation period, a total sample number of 224, 214, 221 and 211 was collected at Beijing, Tianjin, Shijiazhuang and Xinglong, respectively.

15 Detailed records of the instrumental conditions were preserved during sampling, including the sampling time, the sampled-air volume, atmospheric pressure, air temperature, etc. After sampling, the quartz filters were individually placed in petri dishes and immediately stored at $-20 \text{ }^\circ\text{C}$ prior to weighing and subsequent analysis. To ensure that the instrument worked at the specified flow rate, the airflow rate of the sampler was calibrated before and after each sampling.
20 The carbon brush was replaced every month, and the outlet of the tail pipe was kept far away from the sampler in order to avoid contaminating filter samples. During the sampling process, strict quality control was conducted to avoid any pollution. The frequent cleaning of the cutter and tray of the membrane was basic and necessary.

2.2 Chemical analysis

2.2.1 Gravimetry

25 The quartz fiber filters, which were packaged with aluminum foil, were prepared in a muffle



furnace at 500°C for 4 h to remove organic materials. In addition, in order to minimize the influence of water adsorption, the filters were weighed before and after sampling using a microelectronic balance with a reading precision of 10 µg after undergoing a 48 h equilibration period inside a chamber under conditions of constant temperature (20±1 °C) and humidity (45±5%). Atmospheric PM_{2.5} masses were deduced from the gravimetric measurements performed before and after sampling. To guarantee the accuracy of the weighing, weighing was repeated until a difference between two measured weights of below 0.10 mg was achieved. All procedures were strictly quality-controlled to avoid any possible contamination of the samples.

2.2.2 Chemical analysis

10 A quarter of each sample was ultrasonically extracted with using 50 mL deionized water (with a specific resistivity of 18.2 MΩ/cm) for 30 min. After passing through microporous membranes with a pore size of 0.22 µm, the extracted solutions were analyzed using an ion chromatograph (IC) system (Dionex ICS-90, USA) for the detection of SO₄²⁻, NO₃⁻, NH₄⁺, Cl⁻, K⁺, Na⁺, Ca²⁺ and Mg²⁺. More details are given by Huang et al. (2016).

15 A 0.495 cm² punch split from another quarter of each sample was used for the analysis of organic carbon (OC) and elemental carbon (EC), which was performed using a thermal/optical carbon aerosol analyzer (DRI Model 2001A, Desert Research Institute, USA) following the protocol of IMPROVE_A (TOR). Detailed procedures can be found in Cao et al. (2005) and Li et al. (2012).

20 The microwave acid digestion method was used to digest filter samples into liquid solution for elemental analysis. One quarter of each filter sample was placed in the digestion vessel with a mixture of 6 mL HNO₃, 2 mL H₂O₂ and 0.6 mL HF, and then was exposed to a three-stage microwave digestion procedure by a microwave-accelerated reaction system (MARS, CEM Corporation, USA). After that, the digestion solution was transferred to PET bottles and diluted to 25 50 mL with deionized water (with a conductivity of 18.2 MΩ/cm). Agilent 7500a inductively coupled plasma mass spectrometry (ICP-MS, Agilent Technologies, Tokyo, Japan) was used to determine the concentrations of 18 trace elements (TEs) in the digestion solution, including Mg, Al, K, Ca, V, Cr, Mn, Fe, Co, Ni, Cu, Zn, As, Se, Ag, Cd, Tl and Pb). More detailed information, such as instrument optimization, calibration and quality control, is given by Wang et al. (2016b).

2.3 Data analysis method

2.3.1 Chemical mass closure

The chemically reconstructed PM_{2.5} mass (PM_{chem}) was calculated to comprise eight categories of chemical species, which can be expressed as follows:

$$[PM_{chem}] = [Organic\ matter] + [EC] + [Mineral\ dust] + [Trace\ metals] + [Sulfate] + [Nitrate] + [Ammonium] + [Chloride]. \quad (1)$$

In estimating organic matter (OM), an OC to OM conversion factor of 1.6 was adopted for



aerosols at urban sites (Cao et al., 2007; Turpin and Lim, 2001) and the regional background site. Although the literature suggests that a higher OC to OM conversion factor of 2.1 is suitable for rural sites (Bressi et al., 2013; Turpin and Lim, 2001), we still used a uniform value of 1.6 for the sake of spatial comparisons. Therefore,

$$5 \quad [\text{OM}] = 1.6 \times [\text{OC}]. \quad (2)$$

The calculation of mineral dust was performed on the basis of crustal element oxides (such as Al_2O_3 , SiO_2 , CaO , Fe_2O_3 , TiO_2 , MnO_2 and K_2O). The content of Ti is very low in atmospheric particulate matter and was usually $0.04 \mu\text{g}/\text{m}^3$ in the atmospheric particles in Beijing, Tianjin and Shijiazhuang (Zhao et al., 2013c). Thus, eliminating the Ti content has an almost negligible
10 influence on the estimation of the mineral dust. Mineral dust was calculated as:

$$[\text{Mineral dust}] = [\text{Al}_2\text{O}_3] + [\text{SiO}_2] + [\text{CaO}] + [\text{MnO}_2] + [\text{Fe}_2\text{O}_3] + [\text{K}_2\text{O}] = 2.14 \times [\text{Si}] + 1.89 \times [\text{Al}] + 1.4 \times [\text{Ca}] + 1.58 \times [\text{Mn}] + 1.43 \times [\text{Fe}] + 1.21 \times [\text{K}] \quad (3)$$

In this study, the measurement of trace elements in particles did not include the determination of Si, so the content of Si was calculated based on its ratio to Al in crustal materials, namely, $[\text{Si}] = 3.41 \times [\text{Al}]$. The calculations of K_2O and Fe_2O_3 were also based on their ratios to Al in crustal
15 materials, considering that they have abundant artificial sources in addition to natural sources.

The trace metal content reflects the sum of 11 different heavy metal species and was expressed as:

$$[\text{Trace metals}] = \text{V} + \text{Co} + \text{Ni} + \text{Cu} + \text{Pb} + \text{Zn} + \text{As} + \text{Se} + \text{Ag} + \text{Cd} + \text{Tl} \quad (4)$$

The above chemical reconstruction method was applied to the four sites, and the comparison
20 of the reconstructed results (PM_{chem}) with the membrane-weighing results (PM_{grav}) is shown in Figure S1. It can be clearly seen that PM_{chem} is significantly related to PM_{grav} , indicating that the chemical reconstruction method exhibited strong reliability. However, PM_{chem} concentrations at the four sites were all less than those of PM_{grav} , that is to say, there exist unresolved matter that
25 may largely be retaining water in the sampling membrane and particulate matter. Moreover, during the period between weighing and chemical measurement, the volatilization of organic matter and the decomposition of ammonium nitrate may occur. The discrepancy between PM_{chem} and PM_{grav} was thus defined as unknown.

2.3.2 PMF model

The EPA Positive Matrix Factorization (PMF) 5.0 model was applied to apportion the sources
30 of $\text{PM}_{2.5}$ in this study, as it is an effective source apportionment receptor model that has been successfully applied to source apportionment in many cities and regions throughout the entire world (Huang et al., 2014; Reff et al., 2007). Compared to the CMB model (Chemical Mass Balance), the PMF model does not require source profiles prior to analysis, but only requires the
35 values of the concentrations of sample species and their uncertainties (U.S. Environmental Protection Agency, 2014; Zhang et al., 2015c). In this study, model simulations were applied to



datasets composed of 34 species: eight carbon fractions (OC1, OC2, OC3, OC4, OPC, EC1, EC2 and EC3), 8 inorganic species (SO_4^{2-} , NO_3^- , NH_4^+ , K^+ , Na^+ , Ca^{2+} , Mg^{2+} and Cl^-), and 18 inorganic elements (Mg, Al, K, Ca, V, Cr, Mn, Fe, Co, Ni, Cu, Zn, As, Se, Ag, Cd, Tl and Pb). Due to the low OC and EC concentrations at the background site, the entire concentration of OC and EC was input into the PMF model instead of the eight carbon fractions. In addition to the concentrations of the sample chemical species, the uncertainties of the sample species were calculated based on two different situations according to the PMF 5.0 user guide (U.S. Environmental Protection Agency, 2014):

If the concentration is less than or equal to the provided method detection limit (MDL) provided, the uncertainty is calculated using a fixed fraction of the MDL, as $Uncertainty = \frac{5}{6}MDL$.

If the concentration is greater than the provided MDL, the calculation is defined as $Uncertainty = \sqrt{(Error\ Fraction + Concentration)^2 + (0.05MDL)^2}$. In this study, the error fractions of SO_4^{2-} , NO_3^- and NH_4^+ were estimated at 5%, those of OPC, EC2 and EC3 were 15%, and those of other species were 10%.

3. Results and discussion

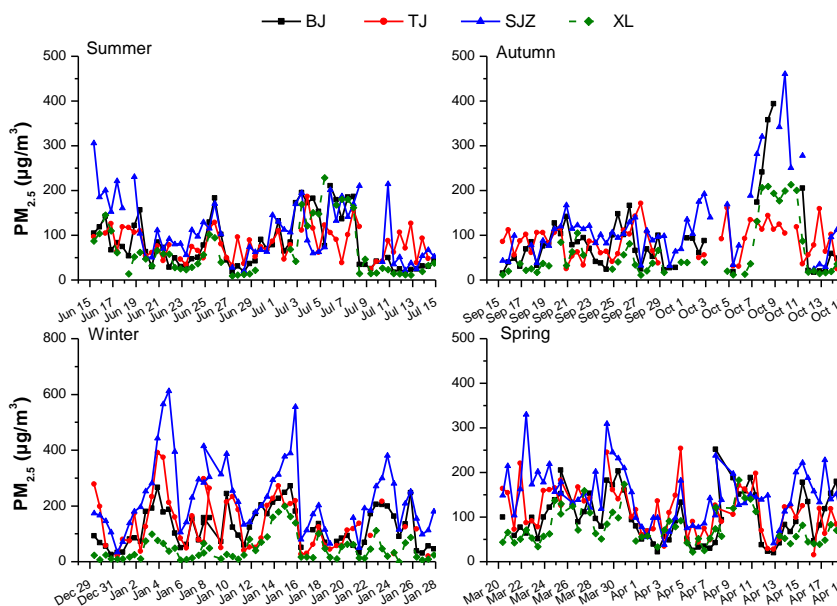
3.1 General characteristics of $\text{PM}_{2.5}$

3.1.1 Annual mass concentrations

Figure 2 reports the temporal variability of the gravimetrically determined $\text{PM}_{2.5}$ concentrations at the four sites (Beijing, Tianjin, Shijiazhuang and Xinglong) throughout the entire observation period. The strong day-to-day variability of $\text{PM}_{2.5}$ concentrations can be easily observed, especially in winter, when $\text{PM}_{2.5}$ ranging from 50.7 to 556.0 $\mu\text{g}/\text{m}^3$ at Shijiazhuang. These concentrations typically record periodic ‘clean-polluted-clean’ cycles for a few days, which were also reported by Guo et al. (2014), who noted that Beijing haze pollution underwent clear periodic cycles of 4–7 days in length. In addition to variations in source emissions and atmospheric processes, these periodic cycles of haze episodes are primarily driven by fluctuations in meteorological conditions (Guo et al., 2014; Zhang et al., 2015b), such as wind speed, relative humidity, air temperature/pressure, atmospheric stability, the height of the planetary boundary layer and air mass origins. Very similar patterns of $\text{PM}_{2.5}$ temporal variations were found at all four sites (Fig. 2), suggesting the homogeneous characteristics of atmospheric particulate matter on a regional scale. On average, the $\text{PM}_{2.5}$ annual concentrations throughout the entire observation period recorded higher levels at urban sites, which were 99.5, 105.7, 155.2 $\mu\text{g}/\text{m}^3$ at Beijing, Tianjin and Shijiazhuang, respectively, and represented values that were 1.5, 1.6 and 2.4 times those at the background site (Xinglong), respectively. This was particularly serious at Shijiazhuang, which consumes huge amounts of energy for industrial processes and daily life (Zhao et al.,



2013b); during the entire observation period, 81% of samples at Shijiazhuang exceeded the second grade of the PM_{2.5} daily average mass concentration in China (75 µg/m³), followed by Tianjin (63%) and Beijing (55%). In contrast, at Xinglong, only 29% of the total samples exceeded 75 µg/m³, which may have mainly resulted from regional transport of pollutants from polluted areas.



5

Figure 2. Time-series of gravimetric PM_{2.5} concentrations during the four study periods

3.1.2 Seasonality

Due to the minor effects of anthropogenic emissions, the seasonal variations of PM_{2.5} concentration at Xinglong were not significant (56.7-77.9 µg/m³), and only slightly higher values were observed in spring. Zhao et al. (2009) also determined that maximum PM_{2.5} concentrations usually occur during spring in Shangdianzi, which is another regional background area in the North China Plain. However, at urban sites, significant seasonal variations were observed, especially at Shijiazhuang. The highest PM_{2.5} values were recorded in winter, with average concentrations of 124.8, 136.6 and 231.8 µg/m³ at Beijing, Tianjin and Shijiazhuang, respectively. A large number of studies have also revealed that the heaviest haze pollution, with extremely high PM_{2.5} loading, occurs in winter in the BTH region (Wang et al., 2012a; Zhang and Cao, 2015), which has mainly been attributed to the combination of intensive coal-fired heating and unfavorable meteorological conditions (i.e., more frequent occurrences of stagnant weather, temperature inversion and low boundary layer height) in this region (Tang et al., 2016a; Zhang and Cao, 2015; Zhao et al., 2009). Following winter, the average PM_{2.5} concentrations in spring also remained at a relative high level at urban sites (101.0-148.4 µg/m³), which may have partly

15

20



resulted from the enhanced mineral dust (see Fig. 5) produced by relatively high wind speeds during this season (Table S1). Due to strong turbulence occurring under conditions of strong radiation intensity and high temperature in summer, as well as the high atmospheric mixing layer generally observed in this season (Tang et al., 2016a), air pollutants could have been effectively diluted and diffused to some extent and thus resulted in the lowest measured PM_{2.5} concentration during this season. In all four seasons, the PM_{2.5} concentrations at Shijiazhuang were significantly higher than those at Beijing and Tianjin. In addition to intensity of the source emissions, meteorological parameters played an important role in this difference between sites, as Shijiazhuang recorded relatively high relative humidity and low wind speeds, which were both beneficial to the accumulation of PM_{2.5} mass (Liu et al., 2017). Furthermore, the largest difference in the PM_{2.5} average mass concentrations between urban sites and the background site occurred in winter, yielding values of 2.2-4.1 times those at Xinglong. This spatial difference could be explained by the strong intensity of pollution emissions in winter at urban sites.

3.2 Chemical components

3.2.1 Annual compositions

The chemical compositions of the entire sample set collected from the three urban sites and the regional background site were also similar, thus again confirming the regional homogeneity of atmospheric PM_{2.5}. The compositions of PM_{2.5} in this region (Fig. 3) were primarily composed of organic matter (OM=OC×1.6, 16.0%-25.0%), secondary inorganic aerosols (SIA, including sulfate, nitrate and ammonium, 43.6%-53.1%), mineral dust (14.7%-20.8%); and lower proportions of EC (2.8%-6.2%), chloride (1.9%-5.5%), and trace metals (0.4%-0.6%). The annual average concentrations of carbonaceous aerosols (OM plus EC) were 31.1, 27.0 and 44.2 μg/m³ at Beijing, Tianjin and Shijiazhuang, respectively, thus constituting large fractions (25.5%-31.2%) of PM_{2.5} in the urban atmosphere. It is worth noting that the EC accounted for 6.2%, 5.9% and 5.7% of the mass of PM_{2.5} at Beijing, Tianjin and Shijiazhuang, respectively, which are higher than that measured at Xinglong (2.8%), reflecting the strong emissions from fossil fuel combustion in urban areas. At Xinglong, lower concentrations and lower fractions of organic matter and higher fractions of mineral dust and SIA compared to those of urban sites were discovered. The presence of lower contributions of organic matter but higher contributions of SIA at the background site is consistent with the results measured on Qimu Island (another regional background site in North China, which is located approximately 300 km southeast of the BTH region) from 3 January to 11 February 2014 (Zong et al., 2016). This was mainly attributed to the regional-scale emission characteristics of gaseous precursors in this region, in which there are more abundant SO₂, NO_x, NH₃ emissions than OC emissions (Zhao et al., 2012), and the general characteristics of the regional atmosphere are accurately reflected at the regional background site.

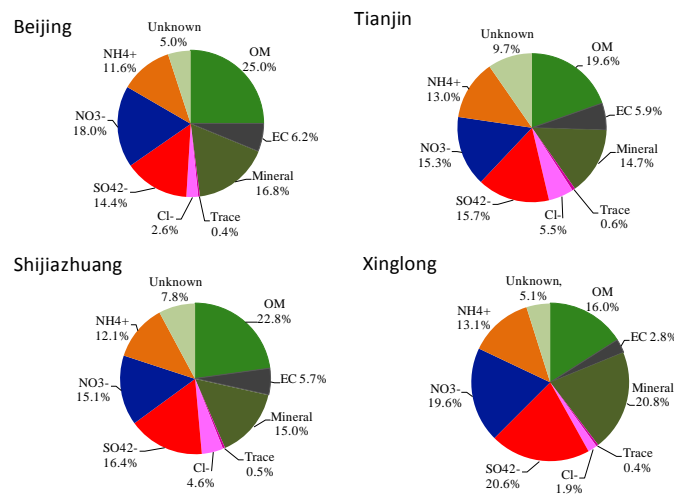


Figure 3. Pie charts depicting the relative contribution of major chemical components of gravimetric PM_{2.5} based on annual data

As the key PM_{2.5} constituents, sulfate, nitrate and ammonium, are generally recognized to originate from the secondary conversion of gaseous SO₂, NO_x and NH₃ through gas-phase chemical reactions and heterogeneous reactions (Wang et al., 2016a; Zhang et al., 2015b). In this study, they accounted for 14.4%-20.6%, 15.1%-19.6% and 11.6%-13.1% of the annual average gravimetric PM_{2.5} concentrations, respectively. Among the three urban sites, the highest NO₃⁻ contribution (18.0%) was found at Beijing, which was in agreement with its strong traffic source. In addition, the mass ratio of NO₃⁻/SO₄²⁻ at Beijing was 1.25, which was higher than that at Tianjin (0.97) and Shijiazhuang (0.92) as well as that at Xinglong (0.95). The NO₃⁻/SO₄²⁻ mass ratio has often been used as an indicator of the relative contributions to aerosol particles from mobile versus stationary sources for sulfur and nitrogen in the atmosphere (Arimoto et al., 1996; Cao et al., 2009; Han et al., 2016), as vehicle exhausts and coal-combustion emissions are significant contributors to nitrate and sulfate, respectively (Huang et al., 2014). Therefore, the NO₃⁻/SO₄²⁻ mass ratio was larger than 1.0 at Beijing, implying that the predominance of motor vehicle emissions over coal combustion in the contribution to PM pollution (Han et al., 2016), while at Tianjin and Shijiazhuang, coal combustion may still play a dominant role. However, compared to the reported results, the NO₃⁻/SO₄²⁻ mass ratios at the two cities also increased from 0.85 (2009-2010) (Zhao et al., 2013b) to 0.92 (this study) at Shijiazhuang, as well as from 0.69 (2008) (Gu et al., 2011) to 0.75 (2009-2010) (Zhao et al., 2013b) and to 0.97 (this study) at Tianjin. This increasing trend also occurred in the background area, as the NO₃⁻/SO₄²⁻ mass ratio at Xinglong increased from 0.78 (2009-2010) (Li, et al., 2013) to 0.95 (this study). These results clearly revealed that atmospheric nitrate pollution is worsening in this region, which is generally

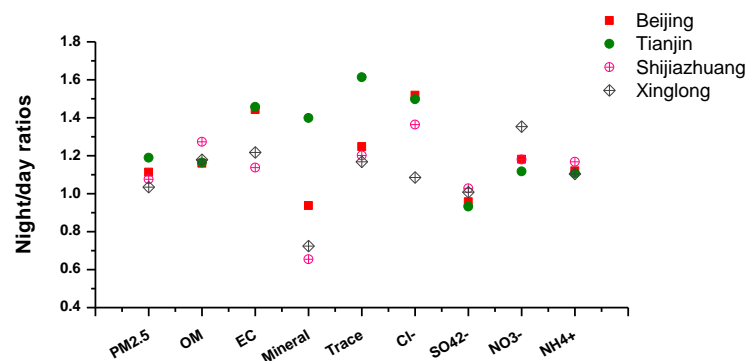


recognized as being caused by increasing motor vehicle emissions and indicates the remarkable effect of the control measures of SO₂ emission.

In addition to carbonaceous and SIA aerosols, mineral dust was also a major component of these aerosols, which constituted a smaller fraction of the PM_{2.5} concentrations (14.7%-16.8%) at urban sites than it did at the background site (20.8%). Cl⁻ exhibited higher concentrations and fractions at Shijiazhuang (7.2 μg/m³, 4.6%) and Tianjin (5.8 μg/m³, 5.5%) than it did at Beijing (2.6 μg/m³, 2.6%) and Xinglong (1.2 μg/m³, 1.9%), further illustrating the important contribution of coal combustion to PM_{2.5} at Shijiazhuang and Tianjin. Trace element concentrations varied from 0.3 to 0.7 μg/m³ and constituted only a minor fraction of PM_{2.5}.

10 3.2.2 Diurnal variation

The analysis of day-night variations indicates that the diurnal difference in the PM_{2.5} annual average concentration was significant at urban sites, where values were 8%-19% higher in the nighttime than they were during the daytime, while negligible diurnal differences were found on the annual scale at Xinglong (Fig. 4). This obvious diurnal variation of PM_{2.5} in urban areas was probably due to the apparent change in the height of the mixing layer between day and night (Zhao et al., 2009). Furthermore, strengthened burning activities may occur at night, as the night/day ratios of EC and Cl⁻, which are both exclusively derived from primary emissions, were higher than those of PM_{2.5}. However, at Xinglong, the dominant source was from regional or long-range transport, with fewer contributions from local emissions; thus, the nocturnal stable boundary layer could have reduced the quantity of transmissions from the outside. Chemical compositions also recorded obvious diurnal variations, as the mass ratio of NO₃⁻/SO₄²⁻ recorded higher values in the nighttime (0.99-1.39) than it did in the daytime (0.81-1.13), which is consistent with similar results obtained by Sun et al. (2016) conducted in Xianghe, which is located approximately 50 km southeast of Beijing. Such diurnal variation indicates the important role of gas-phase photochemical production of sulfate during the daytime, while the facilitated gas-to-particle partitioning of semi-volatile nitrate is associated with the low temperatures (Sun, et al., 2016) and effective hydrolysis of N₂O₅ at night, which is a major source of nitric acid in the urban atmosphere during the nighttime and can occur more efficiently on wet surfaces (Zhang et al., 2015b). In addition, the relatively static and stable meteorological conditions at night resulted in obviously lower fraction of mineral dust (11.3-17.0%, except for Tianjin), compared to those recorded during the daytime (18.3-24.3%).

Figure 4. Day-night variations of PM_{2.5} and its major compositions based on annual data

3.2.3 Seasonal variation of chemical components

The PM mass and its chemical compositions are governed by the chemical processes, evolution of emission sources and meteorological conditions (Bressi et al., 2013; Liu et al., 2017), which usually exhibit seasonality. The seasonal pattern of PM_{2.5} at urban sites was mainly driven by OM, SIA and mineral dust, which were the major components of PM_{2.5} during each season. In winter, the dominant component at urban sites was OM; moreover, from Fig. 5, it can be seen clearly that the OM concentration and its contribution to PM_{2.5} mass were significantly higher in winter (38.1-82.7 $\mu\text{g}/\text{m}^3$, 27.9-35.7%) than in other seasons. In addition, the EC concentration also reached a maximum value in winter at urban sites, yielding values of 11.8, 10.7 and 16.3 $\mu\text{g}/\text{m}^3$ at Beijing, Tianjin, and Shijiazhuang, respectively. Similar seasonal variations of carbonaceous aerosols were also observed in the BTH region (Beijing, Tianjin, Shijiazhuang, Chengde and Shangdianzi) (Zhao et al., 2013), Jinan (Yang et al., 2012) and the Pearl River Delta region (Cao et al., 2004). There are two possible explanations for this phenomenon. On the one hand, a substantial increase in the amount of coal-fires used for residential heating in winter could strengthen the abundance of carbon-containing emissions, including primary organic carbon, EC, and VOCs (Zhao et al., 2012). On the other hand, the lower temperatures in winter could favor the conversion from gaseous VOCs to their particulate form (Wang et al., 2015), whereas the high temperatures in warm seasons, especially in summer (during which the lowest OM concentrations can be seen in Fig. 5), may cause the semi-volatile organic compounds to mainly exist in their gaseous form in the atmosphere. Cl⁻, which is a good tracer of coal combustion, also exhibited higher concentrations and contributions to PM_{2.5} mass in winter (5.3-14.6 $\mu\text{g}/\text{m}^3$, 4.6-6.3%) than it did in other seasons (1.0-5.6 $\mu\text{g}/\text{m}^3$, 1.2-4.9%) at urban sites. However, since it is less affected by local anthropogenic sources, the Xinglong site recorded the lowest concentrations and contributions of EC and Cl⁻, which showed no distinct seasonal variation.

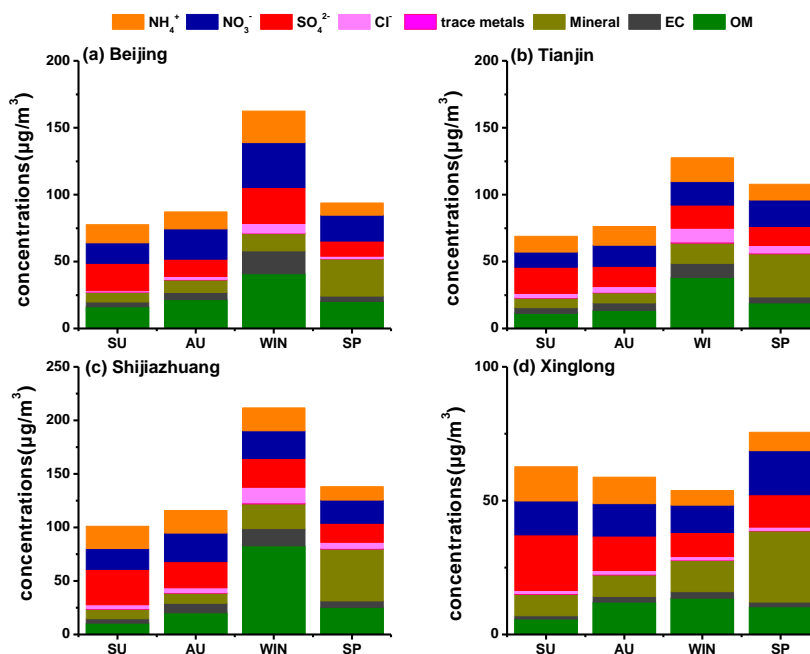


Figure 5. Seasonal variations of the major chemical components in the four sites (SU, AU, WIN, and SP represent the season of summer, autumn, winter and spring, respectively)

Unlike OM, SIA recorded the highest contributions in summer at urban sites (51.7–66.2%), which were significantly higher than those in winter and spring. The prominence of SIA in summer was more apparent at Xinglong (71.2%), which reflected the dominant contributions of meteorological factors. At urban sites, SIA also presented prominent contributions to $\text{PM}_{2.5}$ in autumn (51.9–58.1%) and the average $\text{PM}_{2.5}$ concentration was comparable in summer and autumn, which may have resulted from the high relative humidity in autumn, which is even higher than that in summer (Table S1). However, the contributions of sulfate and nitrate exhibited obvious seasonal differences at these three urban sites and even more apparent differences at the background site, recording greater contributions of sulfate in summer (23.6–29.9%) and nitrate in autumn (18.4–25.7%). This pattern was also found in our previous study in Beijing (Huang et al., 2016). This trend is closely related to their respective chemical/physical properties and mechanisms of generation, as nitrate tends to be decomposed under high temperatures (which mainly occurs in summer) due to the thermodynamic instability of ammonium nitrate, while the process of the chemical generation of ammonium sulfate (i.e., the gas-phase oxidation of SO_2 and subsequent heterogeneous reactions) is largely promoted under the high temperatures and intense solar radiation of summer (Huang et al., 2016; Ianniello et al., 2011; Zhang et al., 2015b).

In spring, the primary chemical component at all four sites was mineral dust, which contributed 27.5–34.1% to $\text{PM}_{2.5}$ and was significantly higher than it was in other seasons



(7.5%-20.7%), thus reflecting the important influence of northwest dust on the atmospheric fine particles of the BTH region in spring and the increase of local resuspended dust (such as road dust and construction dust) resulting from the enhanced wind speed during this season (Table S1).

3.2.4 Chemical variations at different pollution levels

5 By using the PM_{2.5} pollution grading standards of the Air Quality Index (AQI) technical regulations (HJ 633-2012) formulated by the Chinese Ministry of Environmental Protection as a reference, and considering the quantity of samples analyzed in this study, days with average concentrations of PM_{2.5} < 75, 75 ≤ PM_{2.5} < 150 and PM_{2.5} ≥ 150 μg/m³ were defined as clean, moderate pollution and heavy pollution days, respectively. The seasonal distribution of sample
10 quantity at different pollution levels was listed in Table S2. Figure 6 shows the concentrations of chemical compositions and the percentage of the sample quantity at different pollution levels throughout the entire campaign at each site, from which we can see that aerosol pollution was most serious at Shijiazhuang with only 19% at clean level and 42% at heavy pollution level. With the deterioration of pollution, nearly all chemical components increased continuously and
15 noticeably. A remarkable increase of carbonaceous aerosols was observed during the pollution process, in which the average OC and EC concentration on heavy pollution days were 3.5-7.0 and 4.6-5.9 times as high as they were on clean days, respectively. At each pollution level, both OC and EC concentrations were lowest at Xinglong and highest at Shijiazhuang. The OC/EC mass ratio decreased significantly with pollution levels at Beijing, with its value varying from 3.4 (clean
20 days) to 2.7 (moderate pollution days) to 2.1 (heavy pollution days). Tianjin also recorded a similar trend (varying from 2.3 to 2.4 to 1.7, respectively), but this change was less apparent than that at Beijing. As reported by Watson et al. (2001), lower OC/EC ratios are emitted from motor vehicles (1.1) than are emitted from coal combustion (2.7) and biomass burning (9.0). Saarikoski et al. (2008) have also documented OC/EC ratio of 6.6 for biomass burning and 0.71 for traffic
25 emissions. Moreover, the OC/EC ratio for diesel vehicles has been observed much lower value than that for gasoline vehicles (Na et al., 2004). Therefore, we speculate that this pattern of variation of the OC/EC mass ratio at Beijing may be influenced by the strengthened contributions of local motor vehicle exhaust under heavily polluted conditions due to weakened regional transport, which usually contributes most during the initial and growth stages of haze episodes
30 while decreasing during the peak pollution stage, this mechanism has been confirmed in some pollution processes in Beijing (Liu et al., 2016b; Tang et al., 2015a). Therefore, the fact that the OC/EC ratio increases with the increasing development of haze pollution indicates the key role of local traffic emission in the haze progress at Beijing. However, the OC/EC mass ratio increased on heavy pollution days (from 2.2 to 2.7) at Shijiazhuang, indicating that there are different haze
35 formation mechanisms and pollution sources at Shijiazhuang. Different from the key role of local motor vehicle exhaust in the severe haze period at Beijing, at Shijiazhuang, the emissions of coal



combustion may dominate the haze pollution and accumulate constantly. In addition, the secondary formation of SOA from VOCs may be more significant during the pollution process at Shijiazhuang, as the fact that more remarkable increase of OM contribution to $PM_{2.5}$ was observed at this site.

5 In addition, SIA significantly contributed to the enhancement of $PM_{2.5}$ mass during pollution events, from 16.5-29.5 $\mu\text{g}/\text{m}^3$ on clean days to 46.7-77.6 $\mu\text{g}/\text{m}^3$ on moderate pollution days to 91.8-132.7 $\mu\text{g}/\text{m}^3$ on heavy pollution days. Many studies have shown that enhanced heterogeneous reactions under conditions of relatively high humidity are the main reason for the increased SIA during haze periods (Huang et al., 2016; Sun et al., 2013; Wang et al., 2012b). The growth of SIA
10 was particularly important in the haze formation at Beijing and Xinglong, as the SIA contribution increased significantly, from 34.5% on clean days to 44.2% on moderate pollution days to 51.3% on heavy pollution days at Beijing, and from 41.2% to 57.5% to 68.3%, respectively, at Xinglong. At Beijing, among the three secondary inorganic components, only the contribution of nitrate recorded a pronounced increase during the pollution process, thus indicating that haze pollution in
15 Beijing mainly resulted from the secondary transformation of NO_x that was mainly derived from local traffic emissions, and once again reflecting the dominant contribution of local motor vehicle exhaust in haze episodes. In contrast to that observed at Beijing, sulfate, nitrate and ammonium all clearly increased with the deterioration of pollution at Xinglong, suggesting that its high $PM_{2.5}$ loadings mainly resulted from the intensifying secondary transformations of gaseous pollutants
20 (SO_2 , NO_x and NH_3) during stagnant meteorological conditions in the background area. An average increase in the contributions of SIA during the pollution process was not observed at Tianjin and Shijiazhuang, but did occur in all seasons except for spring. The mineral dust contribution increased on heavy pollution days in spring at Tianjin and Shijiazhuang, indicating the important role of soil dust in the formation of spring haze at the two study sites.

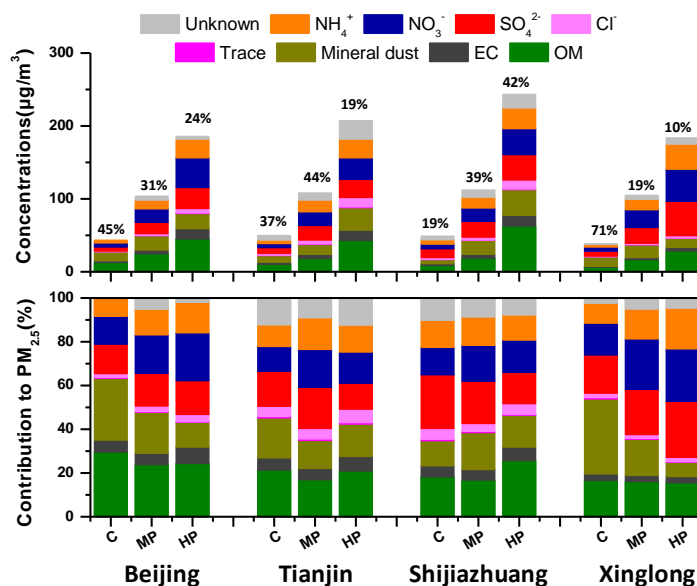


Figure 6. The evolution of chemical components at different pollution levels throughout the entire study period. C, MP, and HP represent clean days ($PM_{2.5} < 75 \mu\text{g}/\text{m}^3$), moderate pollution days ($75 \leq PM_{2.5} < 150 \mu\text{g}/\text{m}^3$) and heavy pollution days ($PM_{2.5} \geq 150 \mu\text{g}/\text{m}^3$), respectively. "%" represents the proportion of filter sample quantity at each pollution level in total samples.

3.3 Source apportionment by PMF

3.3.1 Identified sources

The sources/factors of $PM_{2.5}$ at three urban sites were apportioned by applying the receptor model PMF; this was also performed at Xinglong for comparison. The identification of the sources was based on certain chemical tracers which are generally presumed to be emitted from specific sources and present in significant amounts in the collected samples (Singh et al., 2016). Based on this, eight factors were identified for Beijing and Tianjin, whereas nine were identified for Shijiazhuang and only five were identified for Xinglong. The relative dominance of each source varied by site and season. Contributions of the identified sources determined by analyzing the annual data are shown in Fig. 8; the factor profiles of $PM_{2.5}$ for the regional background site (Xinglong) are listed in Fig. 7, while those for the urban sites are shown in Supplementary Fig. S2-4. These factors can be summarized as follows:

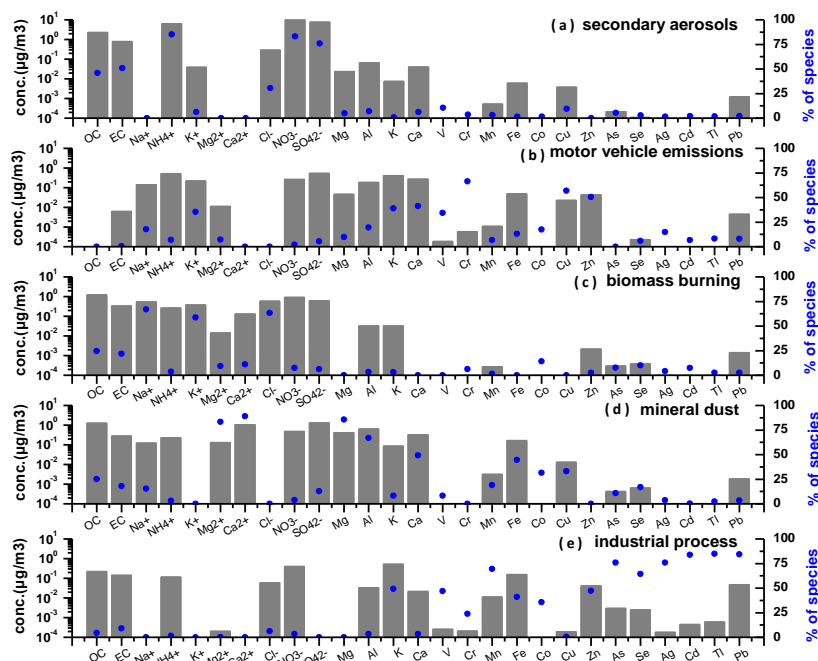


Figure 7. PMF factor/source profiles for $PM_{2.5}$ samples throughout the entire study period at Xinglong in concentration ($\mu\text{g}/\text{m}^3$) and percentage (%)

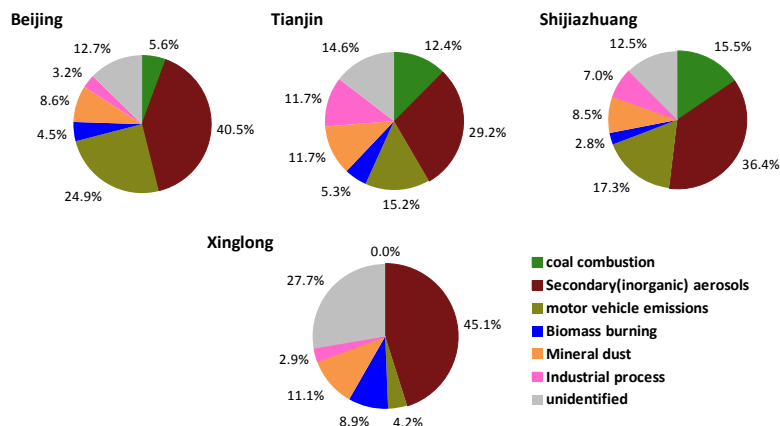


Figure 8. The annual contributions of identified sources to $PM_{2.5}$ mass at the four sites

(i) Coal combustion. In China, coal combustion is generally used in thermal power plants, as well as for winter residential heating in its northern cold regions. This source is characterized by high loadings of OC, EC, and chloride, most of which were apportioned in this factor (Fig. S2-4 a). At the three urban sites, the coal combustion source exhibited significantly higher



concentrations (17.6, 31.6 and 67.8 $\mu\text{g}/\text{m}^3$ at Beijing, Tianjin and Shijiazhuang, respectively) and contributions to $\text{PM}_{2.5}$ (14.1%, 23.3% and 29.2%, respectively) in winter, than were seen in other seasons (which recorded concentrations of 0.6-16.1 $\mu\text{g}/\text{m}^3$ and contributions of 0.7-10.7%). This was strongly aligned with the seasonal characteristics of coal combustion activity in this region.

5 The annual average emissions from coal combustion contributed 5.6% to $\text{PM}_{2.5}$ at Beijing and were even higher at Tianjin (12.4%) and Shijiazhuang (15.6%), but were not identified at Xinglong.

(ii) Secondary aerosols/inorganic aerosols. The dominant source of the four studied sites was secondary inorganic aerosols at three urban sites (29.2%-40.5%) and secondary aerosols at
10 Xinglong (45.1%). At Xinglong, this factor (Fig. 7a) could be identified as secondary aerosols because of its high contributions and accumulations of OC, sulfate, nitrate and ammonium, which caused it to include SIA and SOA. In addition, approximately 30% of total chloride was assigned to this source, indicating that a coal combustion source was included in the secondary aerosol source. However, our above analysis indicates that there were only very minor local coal
15 combustion emissions at Xinglong. Therefore, this can probably be attributed to the regional transport of coal combustion emissions, along with secondary sources.

At Tianjin, high contributions of ammonium, nitrate and sulfate, which comprise most of their mass concentrations, were apportioned in the secondary aerosol factor (Fig. S3b) with only minor OC, thus, we identified this factor as the source of secondary inorganic aerosols. In contrast,
20 at Beijing and Shijiazhuang, secondary inorganic aerosols were further separated into two sources defined as nitrate-rich secondary (Fig. S2b and S4b) and sulfate-rich secondary aerosols (Fig. S2c and S4c), which record the respective characteristics of prominent contributions of ammonium/nitrate and ammonium/sulfate. Consistent with the generating mechanism and seasonal characteristics of nitrate and sulfate, the contribution of nitrate-rich secondary aerosols to
25 $\text{PM}_{2.5}$ had the highest values in autumn, whereas the sulfate-rich secondary aerosols had the highest contribution values in summer at Beijing and Shijiazhuang.

(iii) Motor vehicle emissions. Emissions from motor vehicles are crucial to serious air pollution, especially in economically developed megacities. In our study, the source of motor vehicle emissions, which have high concentrations of OC, EC, and the trace metals of Cu, Zn and
30 Pb and are considered to be characteristic species of brake wear dust and tire wear dust (Karnae and John, 2011; Tian et al., 2016; Zhang et al., 2013), was identified at all four study sites, contributing 24.9% (Beijing), 15.2% (Tianjin) and 17.3% (Shijiazhuang) at the urban sites and only 4.2% at Xinglong. This suggested the important role of motor vehicle exhaust in the urban $\text{PM}_{2.5}$ pollution, especially in Beijing, where the quantity of motor vehicles increased to 5.7
35 million by 2016 (<http://www.chinaidr.com/tradenews/2017-03/111537.html>). Notably, secondary aerosols are mainly produced by the gas-to-particle transformation of SO_2 , NO_x , NH_3 , and VOCs, and motor vehicle exhaust is an important source of the emissions of NO_x and VOCs in urban



areas (Huang et al., 2011; Tang et al., 2016b). Therefore, the actual contributions of motor vehicle emissions to particles should be higher if considering the secondary formation of gaseous exhaust in the atmosphere. Since 2017, vehicular emission standard of China in Phase V (equivalent to European V) has been implemented on a national scale, and has caught up with the developed countries. However, less restrictive standard of oil quality in China than that in Europe and United States is the main reason for the strong motor vehicle emissions, particularly the limits standard of aromatics and alkenes. These two unsaturated hydrocarbon species have an important effect on air quality (Schell et al., 2001), as decreasing alkenes contents can decrease the fire temperature and reduce NO_x emissions (Tang et al., 2015b). A new research also reported that gasoline aromatic hydrocarbons performed an essential role in urban SOA production enhancement and thus significantly affected on ambient PM_{2.5} (Peng et al., 2017). The limits standards of aromatics and alkenes contents in vehicle gasoline are respectively 40% and 28% for China IV implemented since 2014, 40% and 24% for China V since 2017, 35% and 18% for China VI suggested to be implemented in 2019 (<http://www.nea.gov.cn/>). In contrast, the limits standard of 35% for aromatics and 18% for alkenes (European IV) in Europe was implemented since 2005 (Tang et al., 2015b). In addition to lower standards, the phenomenon of substandard oil products also exists, as Tang et al. (2015b) reported that 48.4% of gasoline samples in North China exceeded the limit standard of aromatics (40%).

(iv) Biomass burning. Biomass burning emissions in northern China are mainly produced by the burning of agricultural straw and thus often appear during the farming and harvest seasons and can have a significant impact on the atmospheric chemistry and climate on both a regional and global scale (Duan et al., 2004; Li et al., 2010; Sun et al., 2016). The source profiles of factors defined as biomass burning (Fig. 7c, Fig. S2e, S3d and S4e) were rich in K⁺, which is widely regarded to be a good tracer of biomass burning sources. In addition to K⁺, the fresh smoke plumes of burning biomass also contain a significant amount of Na⁺, Cl⁻, OC and EC (Wang et al., 2013a), which were also found in the profile of biomass burning in this study. The annual average contribution of biomass burning to PM_{2.5} exhibited higher values at Xinglong (8.9%) than it did at the three urban sites (2.8%-5.3%). In addition to its high proportion during the harvest season (autumn, 11.6%), biomass burning emissions exhibited their highest contributions to PM_{2.5} in winter at Xinglong (14.6%) and recorded low values (1.0%-4.4%) in winter at the three urban sites. This can likely be attributed to the fact that a single type of fuels is used by the surrounding residents, as bio-fuels (i.e., straw and dry wood) are always utilized for cooking and winter heating (Zhao et al., 2012), which is totally different than the matter used for energy (mainly coal and natural gas) by urban and suburban residents. Similar to the motor vehicle source, the contribution of biomass burning would be higher if considering its emissions of secondary aerosol precursors (VOCs, SO₂ and NO_x), especially VOCs (Bo et al., 2008; Li et al., 2014; Yuan et al., 2010).

(v) Mineral dust. Road dust from local traffic and construction activities (with abundant



concentrations of Mg^{2+} , Ca^{2+} and motor vehicle-related species such as Cu, Zn and Pb) (Han et al., 2007) and soil dust, which is mainly derived from long-range transport (and is more enriched in Al, Ca, Fe, Mg and Mn) were summarized as mineral dust. This source was found to have obvious seasonality, exhibiting its highest contributions in spring at urban sites (17.2%-21.0%) and the background site (22.2%). Influenced by dust from the northwest, this seasonal variation was most significant and regular for soil dust. The factor of road dust was identified at the three urban sites, which contributed annual average values of 3.5%-7.8% to $PM_{2.5}$, but was not extracted from mineral dust at Xinglong due to the minor influence of anthropogenic sources.

(vi) Industrial process. A striking feature of this source was its relatively high concentrations of mining-related elements, such as V, Mn and Fe, and elements related to pollution produced by industrial processes, including As, Se, Ag, Cd, Tl and Pb. More than 50% of the mass concentrations of the above pollution elements were allocated in the source. The annual average emissions from industrial processes contributed 3.2%-11.7% to $PM_{2.5}$ at urban sites, which was lowest at Beijing. The industrial process source (2.9%) at Xinglong may have resulted from the regional transport from regional cities with heavy industrial activity. At Tianjin and Shijiazhuang (two heavily industrial cities), an oil refining/metal smelting source, characterized by high concentrations of V, Mn, Fe, Co and Ni (Mohiuddin et al., 2014), was extracted from the emission source of industrial processes, contributing 2.8% (Tianjin) and 0.7% (Shijiazhuang) to $PM_{2.5}$.

3.3.2 Clean days versus hazy days

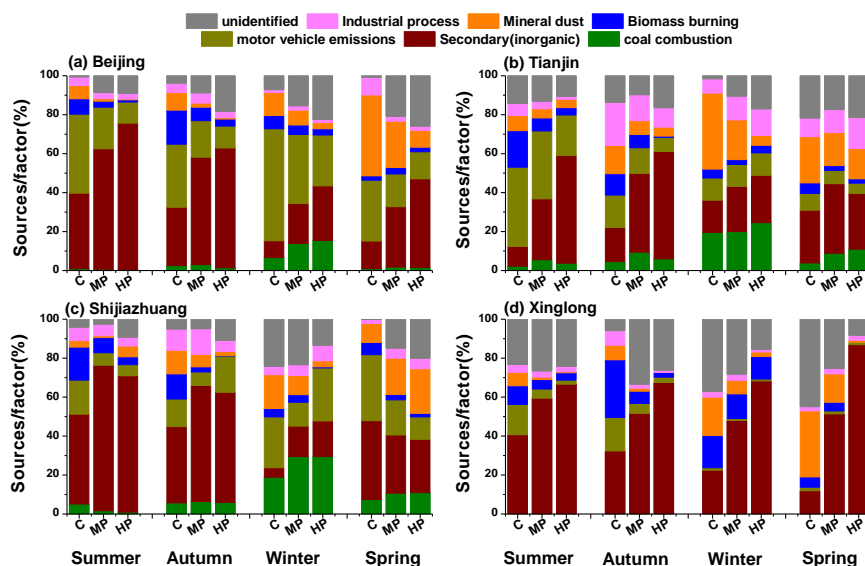
During the transition from clean to pollution processes, significant variations in the contributions of sources/factors contribution were observed, which exhibited strong seasonal features and spatial heterogeneity (Fig. 9). However, the common characteristic in each season or site was that secondary aerosols/inorganic aerosols played a key role in the development of haze pollution, which generally recorded increasing contributions with worsening pollution (except in spring at Shijiazhuang), which was also reported by Huang et al. (2014). Especially in summer and autumn, the source of secondary inorganic aerosols increased most dramatically as a function of high relative humidity and suitable temperature at urban sites; on heavy pollution days, it accounted for 55.7%-75.2% of $PM_{2.5}$ in summer and 55.0%-61.5% in autumn, thus representing the biggest source of atmospheric $PM_{2.5}$ during these two seasons. In contrast, at Xinglong, the secondary aerosols source was always the dominant factor in haze formation, which accounted for 66.7%, 67.5%, 68.4% and 87.0% of $PM_{2.5}$ on heavy pollution days in summer, autumn, winter and spring, respectively. In addition, biomass burning was also another important source during the winter pollution process at Xinglong.

In contrast to background site, the emission sources and generation mechanism of haze pollution were more complex at urban sites, especially in winter, as primary emissions such as motor vehicle emissions, coal combustion and industrial processes were also the main sources of



heavy pollution in winter. As the main fuel for winter heating in the North China Plain, the contribution of coal combustion to $PM_{2.5}$ mainly occurred in winter and was key to the heavy pollution in winter in urban areas, as it increased with increasing pollution levels. Especially at Tianjin and Shijiazhuang, it contributed nearly 30% to $PM_{2.5}$ on heavy pollution days and contributed even more if considering the secondary formation of sulfate from the SO_2 that was largely emitted by coal combustion. Moreover, the primary emissions of motor vehicles also exerted a remarkable impact on the winter haze pollution, accounting for 25.5% and 23.2% of $PM_{2.5}$ on heavy pollution days at Beijing and Shijiazhuang, respectively, and accounting for more if considering the secondary conversion of gaseous pollutants in the vehicle exhaust. Especially on hazy days, low visibility could aggravate urban traffic congestion during rush hour, thus causing more pollutants to be emitted by motor vehicles when operating in this condition (Zhang et al., 2011).

In spring, the effect of mineral dust was also highlighted at urban sites. Most notably, at Shijiazhuang, mineral dust significantly contributed to the aerosol pollution process, as its contribution to $PM_{2.5}$ continuously increased from 9.7% on clean days to 18.6% on moderate pollution days to 22.9% on heavy pollution days. However, along with the increase in pollution levels, the ratio of local road dust in mineral dust decreased from 81.6% (on clean days) to 50% (on pollution days), thus reflecting the significant impact of long-range transported northwest dust on the spring aerosol pollution at Shijiazhuang.



20

Figure 9. Fractional contribution of sources/factors to $PM_{2.5}$ mass at different pollution levels during each season at Beijing (a), Tianjin (b), Shijiazhuang (c) and Xinglong (d)



3.4 Backward trajectory

A 48 h backward trajectory analysis with a 12 h interval using the hybrid single-particle Lagrangian integrated trajectory (HYSPLIT 4.9) model was conducted at all four sites. To reveal the pollution patterns and source signals of $PM_{2.5}$ carried by air masses from different directions and regions, the source contributions of $PM_{2.5}$ were grouped according to their trajectory clusters, as shown in Fig. 10. The results in Fig. 10 indicate the important effect of regional transport on the $PM_{2.5}$. More than half of the air masses (54%, 64%, 51% and 56% for Beijing, Tianjin, Shijiazhuang and Xinglong, respectively) throughout the entire study period were from the BTH region and Shandong Province. These air masses, which move with weak speeds and at low heights could have carried abundant atmospheric pollutants (i.e., particles and gaseous pollutants) from the areas through which they passed, which may have been accompanied by plenty of water vapor during transport (Tao et al., 2012; Zhu et al., 2016), resulting in high $PM_{2.5}$ mass concentrations driven by the local secondary formations at the sampling sites. The air masses (cluster 1 at each site) from the southern direction caused the most serious pollution. Air masses originating from Mongolia were also dominant (27%-46%) in this region (cluster 2-3 at Beijing, cluster 4-5 at Tianjin, cluster 3-4 at Shijiazhuang and cluster 3 at Xinglong), especially in winter, and $PM_{2.5}$ in these clusters were generally lower than those from the surrounding polluted areas, except for Shijiazhuang and Tianjin in cluster 5 (Fig. 10b). In addition, a small proportion of air masses originating from the Hulunbuir prairie in Inner Mongolia, such as cluster 3 at Tianjin and cluster 4 at Xinglong, could have carried clean air to the sampling sites, thus causing the corresponding $PM_{2.5}$ mass concentrations to be the lowest. In contrast to other sites, high average $PM_{2.5}$ concentrations in each cluster were observed at Shijiazhuang, especially in cluster 2, which originated from Inner Mongolia and passed over Shanxi Province before arriving at the sampling sites, and corresponded to be highest $PM_{2.5}$ value ($178.9 \mu\text{g}/\text{m}^3$). Although cluster 4 originated from Mongolia and traveled with fast speed and great height, the $PM_{2.5}$ was indeed higher than that of cluster 1, which may be because it passed over Inner Mongolia and Shanxi Province and thus could have carried many pollutants from these polluted areas. The $PM_{2.5}$ concentration in cluster 3, which originated from Mongolia and passed over Inner Mongolia and northern Hebei (a relatively clean area in the BTH region), was relatively lower ($102.1 \mu\text{g}/\text{m}^3$). However, the heavy pollution at Shijiazhuang was mainly dominated by cluster 1 (51%) from the south, as cluster 2 and cluster 4 accounted for only 23% and 13% of the trajectories, respectively. Similarly, haze pollution at Beijing, Tianjin and Xinglong also developed due to the presence of weak southerly air masses from heavily polluted regions. This is consistent with the results of Guo et al. (2014) and Li et al. (2015).

In addition to the different $PM_{2.5}$ concentrations in different clusters, large differences in the source contributions were also found. For example, at Shijiazhuang, high $PM_{2.5}$ concentrations was observed in each cluster. However, it could also be clearly seen that the source contribution



charts of these clusters were very different, and that the air masses originating from the BTH region and Shandong Province were characterized by high contributions of secondary inorganic aerosols, while air masses from long-range transport were more enriched in mineral dust. Therefore, at Shijiazhuang, the contributions of secondary inorganic aerosols was occurred in the sequence of cluster 1 > cluster 2 > cluster 3 > cluster 4, whereas those of mineral dust exhibited the opposite pattern. Similar patterns were also observed at Xinglong, Beijing and Tianjin in this study. This pattern of secondary inorganic aerosols was also observed by Zhang et al. (2014) in their study in Beijing. As mentioned in Section 3.1, secondary aerosols were primarily attributed to the transformations of their precursors (SO₂, NO_x, NH₃ and VOCs). The slow and near-ground air masses originating from regional polluted areas could have resulted in stagnant conditions, which could have been conducive to the accumulation of precursors from local emissions and transported in, and to the following secondary transformation. Furthermore, during this transportation, the carried gaseous pollutants also could have undergone secondary transformations and directly resulted in a rapid increase in PM_{2.5} concentrations in the downwind area (Bressi et al., 2014; Li et al., 2015). Our previous study also have revealed that the high concentrations of organic aerosols (OA) in Beijing, especially low-volatility oxygenated aerosols that are more oxidized and aged, were associated with southerly originated air masses containing secondary regional pollutants (Zhang et al., 2015a).

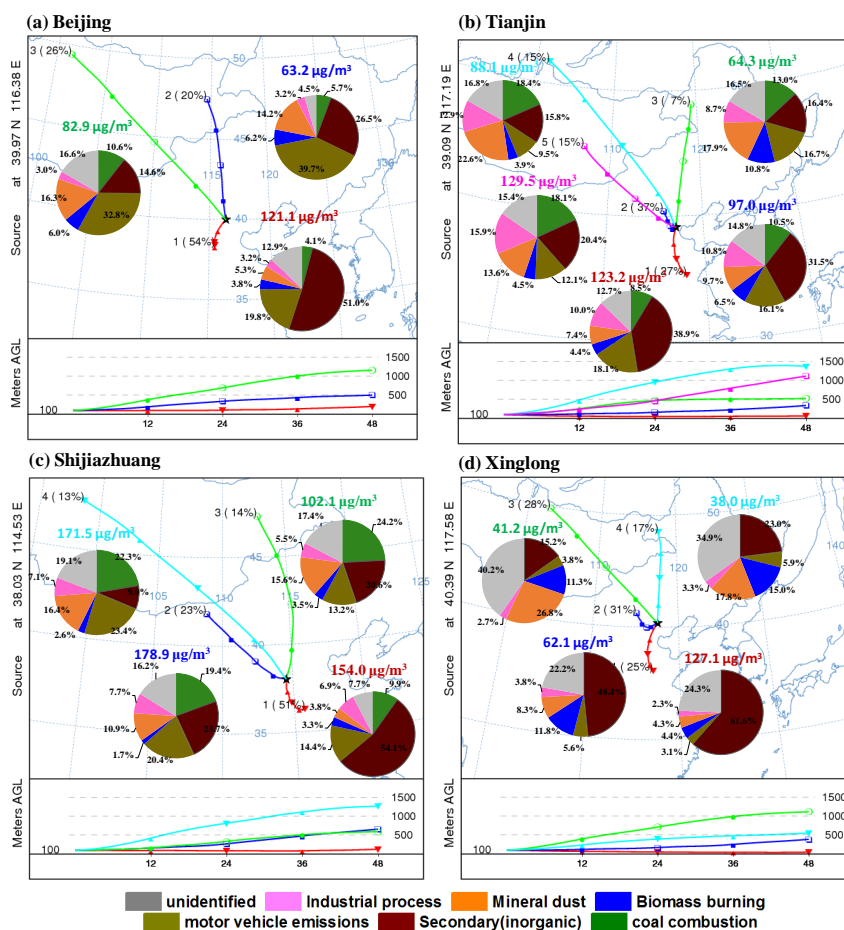


Figure 10. Source contributions resolved from PMF at each 48 h backward trajectory cluster during the entire study period at Beijing (a), Tianjin (b), Shijiazhuang (c) and Xinglong (d)

4. Conclusions

5 In this study, the chemical compositions and emission sources of fine particulate matter (PM_{2.5}) were comprehensively investigated in three urban sites (Beijing, Tianjin and Shijiazhuang) and a background site (Xinglong) at the Beijing-Tianjin-Hebei region. The temporal variations of PM_{2.5} and its chemical components recorded homogeneous features at the four sites, reflecting the regional characteristics of aerosol pollution. However, obvious seasonal and spatial variability of

10 PM_{2.5} and its chemical compositions was observed. Severe PM_{2.5} pollution was found at urban sites, especially at Shijiazhuang, and relatively clean at background site. The seasonal variation of PM_{2.5} concentration at Xinglong was not significant due to the presence of fewer anthropogenic emissions; at urban sites, the lowest PM_{2.5} value was observed in summer and the highest value was observed in winter, likely due to the prevalence of winter coal-fired heating and unfavorable



meteorological conditions. In terms of chemical compositions, the major chemical components in this region were organic matter (16.0%-25.0%), sulfate (14.4%-20.6%), nitrate (15.1%-19.6%), ammonium (11.6%-13.1%), mineral dust (14.7%-20.8%) and its minor components were EC (2.8%-6.2%), chloride (1.9%-5.5%), and trace metals (0.4%-0.6%). These chemical components exhibited their own seasonal and diurnal variation characteristics which were closely related to chemical processes, emission sources and meteorological conditions.

The PMF model-resolved source analysis showed that coal combustion, motor vehicle emissions, secondary inorganic aerosols, mineral dust and industrial processes were the main sources of PM_{2.5} in urban areas; however, the dominant source at the background site was secondary aerosols. The drastic secondary formation of gas precursors was the dominant cause of aerosol pollution, especially in summer and autumn. In winter, coal combustion exerted an important impact on the haze formation in urban areas; in spring, mineral dust also exerted a significant impact. In urban atmospheres, especially in Beijing, the contribution of motor vehicle emissions was also prominent in haze formation, as it is the major source of gaseous NO_x. However, in this study, we could not determine the exact contribution of the secondary transformation of NO_x emitted by motor vehicles. Future studies should be further investigated of additional details about these secondary aerosols.

Haze pollution has remarkable regional characteristics, severe pollution in BTH region was mainly influenced by the region itself and surrounding polluted areas of the south. Therefore, we question the efficiency of the abatement strategies of the emission reduction and air quality improvement and request a joint collaboration of cities in this region, even throughout all of northern China. Emission reduction of gaseous precursors from fossil fuel combustion, especially from motor vehicles by improving oil quality, are essential to mitigate the severe haze pollution in BTH region.

25

Acknowledgements:

This study was supported by the “Strategic Priority Research Program” of the Chinese Academy of Sciences (XDB05020000) and the Ministry of Science and Technology of China (No. 2016YFC0202700). The authors acknowledge the NOAA Air Resource Laboratory for unrestricted provision of HYSPLIT trajectory model. We are also thankful to China Meteorological Administration for the meteorological data.

30

References

Arimoto, R., Duce, R. A., Savoie, D. L., Prospero, J. M., Talbot, R., Cullen, J. D., Tomza, U., Lewis, N. F. and Ray, B. J.: Relationships among aerosol constituents from Asia and the North Pacific during PEM-West A, *J. Geophys. Res. Atmos.*, 101(D1), 2011–2023, doi:10.1029/95JD01071, 1996.



- Bo, Y., Cai, H. and Xie, S. D.: Spatial and temporal variation of historical anthropogenic NMVOCs emission inventories in China, *Atmos. Chem. Phys.*, 8(23), 7297–7316, doi:10.5194/acp-8-7297-2008, 2008.
- 5 Bressi, M., Sciare, J., Ghersi, V., Bonnaire, N., Nicolas, J. B., Petit, J. E., Moukhtar, S., Rosso, A., Mihalopoulos, N. and Féron, A.: A one-year comprehensive chemical characterisation of fine aerosol (PM_{2.5}) at urban, suburban and rural background sites in the region of Paris (France), *Atmos. Chem. Phys.*, 13(15), 7825–7844, doi:10.5194/acp-13-7825-2013, 2013.
- Bressi, M., Sciare, J., Ghersi, V., Mihalopoulos, N., Petit, J. E., Nicolas, J. B., Moukhtar, S., Rosso, A., Féron, A., Bonnaire, N., Poulakis, E. and Theodosi, C.: Sources and geographical origins of fine aerosols in Paris (France), *Atmos. Chem. Phys.*, 14(16), 8813–8839, doi:10.5194/acp-14-8813-2014, 2014.
- 10 Cai, W., Li, K., Liao, H., Wang, H. and Wu, L.: Weather conditions conducive to Beijing severe haze more frequent under climate change, *Nat. Clim. Chang. Press*, (March), doi:10.1038/NCLIMATE3249, 2017.
- 15 Cao, J. J., Lee, S. C., Ho, K. F., Zou, S. C., Fung, K., Li, Y., Watson, J. G. and Chow, J. C.: Spatial and seasonal variations of atmospheric organic carbon and elemental carbon in Pearl River Delta Region, China, *Atmos. Environ.*, 38(27), 4447–4456, doi:10.1016/j.atmosenv.2004.05.016, 2004.
- Cao, J. J., Wu, F., Chow, J. C., Lee, S. C., Li, Y., Chen, S. W., An, Z. S., Fung, K. K., Watson, J. G., Zhu, C. S. and Liu, S. X.: Characterization and source apportionment of atmospheric organic and elemental carbon during fall and winter of 2003 in Xi'an, China, *Atmos. Chem. Phys.*, 5, 3127–3137, doi:SRef-ID: 1680-7324/acp/2005-5-3127, 2005.
- 20 Cao, J. J., Lee, S. C., Chow, J. C., Watson, J. G., Ho, K. F., Zhang, R. J., Jin, Z. D., Shen, Z. X., Chen, G. C., Kang, Y. M., Zou, S. C., Zhang, L. Z., Qi, S. H., Dai, M. H., Cheng, Y. and Hu, K.: Spatial and seasonal distributions of carbonaceous aerosols over China, *J. Geophys. Res.*, 112(D22), doi:10.1029/2006jd008205, 2007.
- 25 Cao, J. J., Shen, Z. X., Chow, J. C., Qi, G. W. and Watson, J. G.: Seasonal variations and sources of mass and chemical composition for PM₁₀ aerosol in Hangzhou, China, *Particuology*, 7(3), 161–168, doi:10.1016/j.partic.2009.01.009, 2009.
- Chen, D., Liu, X., Lang, J., Zhou, Y., Wei, L., Wang, X. and Guo, X.: Estimating the contribution of regional transport to PM_{2.5} air pollution in a rural area on the North China Plain, *Sci. Total Environ.*, 583, 280–291, doi:10.1016/j.scitotenv.2017.01.066, 2017.
- 30 Cheng, Y. F., Zheng, G. J., Wei, C., Mu, Q., Zheng, B., Wang, Z. B., Gao, M., Zhang, Q., He, K. B., Carmichael, G., Po schl, U. and Su, H.: Reactive nitrogen chemistry in aerosol water as a source of sulfate during haze events in China, *Sci. Adv.*, 2(12), e1601530, doi:10.1126/sciadv.1601530, 2016.
- 35 Du, Z., He, K., Cheng, Y., Duan, F., Ma, Y., Liu, J., Zhang, X., Zheng, M. and Weber, R.: A yearlong study of water-soluble organic carbon in Beijing I: Sources and its primary vs. secondary nature, *Atmos. Environ.*, 92, 514–521, doi:10.1016/j.atmosenv.2014.04.060, 2014.
- Duan, F., Liu, X., Yu, T. and Cachier, H.: Identification and estimate of biomass burning contribution to the urban aerosol organic carbon concentrations in Beijing, *Atmos. Environ.*, 38(9), 1275–1282,



- doi:10.1016/j.atmosenv.2003.11.037, 2004.
- Elliot, A. J., Smith, S., Dobney, A., Thornes, J., Smith, G. E. and Vardoulakis, S.: Monitoring the effect of air pollution episodes on health care consultations and ambulance call-outs in England during March/April 2014: A retrospective observational analysis, *Environ. Pollut.*, 214(July), 903–911, doi:10.1016/j.envpol.2016.04.026, 2016.
- 5 Gu, J., Bai, Z., Li, W., Wu, L., Liu, A., Dong, H. and Xie, Y.: Chemical composition of PM_{2.5} during winter in Tianjin, China, *Particuology*, 9(3), 215–221, doi:10.1016/j.partic.2011.03.001, 2011.
- Guo, S., Hu, M., Zamora, M. L., Peng, J., Shang, D., Zheng, J., Du, Z., Wu, Z., Shao, M., Zeng, L., Molina, M. J. and Zhang, R.: Elucidating severe urban haze formation in China., *Proc. Natl. Acad. Sci. U. S. A.*, 111(49), 17373–8, doi:10.1073/pnas.1419604111, 2014.
- 10 Han, B., Zhang, R., Yang, W., Bai, Z., Ma, Z. and Zhang, W.: Heavy haze episodes in Beijing during January 2013: Inorganic ion chemistry and source analysis using highly time-resolved measurements from an urban site, *Sci. Total Environ.*, 544, 319–329, doi:10.1016/j.scitotenv.2015.10.053, 2016.
- Han, L., Zhuang, G., Cheng, S., Wang, Y. and Li, J.: Characteristics of re-suspended road dust and its impact on the atmospheric environment in Beijing, *Atmos. Environ.*, 41(35), 7485–7499, doi:10.1016/j.atmosenv.2007.05.044, 2007.
- 15 He, H., Wang, Y. S., Ma, Q. X., Ma, J. Z., Chu, B. W., Ji, D., Tang, G. Q., Liu, C., Zhang, H. X. and Hao, J. M.: Mineral dust and NO_x promote the conversion of SO₂ to sulfate in heavy pollution days, *Sci. Rep.*, 4(2), 1–6, doi:10.1038/srep04172, 2014.
- 20 Hu, W., Hu, M., Hui, W., Jimenez, J. L., Yuan, B., Chen, W., Wang, M., Wu, Y., Chen, C., Wang, Z., Peng, J., Zeng, L. and Shao, M.: Chemical composition, sources, and aging process of submicron aerosols in Beijing: Contrast between summer and winter, *J. Geophys. Res. Atmos.*, 121(4), 1955–1977, doi:10.1002/2015JD024020, 2016.
- Huang, C., Chen, C. H., Li, L., Cheng, Z., Wang, H. L., Huang, H. Y., Streets, D. G., Wang, Y. J., Zhang, G. F. and Chen, Y. R.: Emission inventory of anthropogenic air pollutants and VOC species in the Yangtze River Delta region, China, *Atmos. Chem. Phys.*, 11(9), 4105–4120, doi:10.5194/acp-11-4105-2011, 2011.
- 25 Huang, K., Zhuang, G., Lin, Y., Li, J., Sun, Y., Zhang, W., Fu, J. S., Huang, K., Zhuang, G., Lin, Y., Li, J., Sun, Y., Zhang, W. and Fu, J. S.: Relation between optical and chemical properties of dust aerosol over Beijing, China, *J. Geophys. Res.*, 115, 0–16, doi:10.1029/2009JD013212, 2010.
- 30 Huang, R. J., Zhang, Y., Bozzetti, C., Ho, K. F., Cao, J. J., Han, Y., Daellenbach, K. R., Slowik, J. G., Platt, S. M., Canonaco, F., Zotter, P., Wolf, R., Pieber, S. M., Bruns, E. A., Crippa, M., Ciarelli, G., Piazzalunga, A., Schwikowski, M., Abbazade, G., Schnelle-Kreis, J., Zimmermann, R., An, Z., Szidat, S., Baltensperger, U., El Haddad, I. and Prevot, A. S.: High secondary aerosol contribution to particulate pollution during haze events in China, *Nature*, 514(7521), 218–222, doi:10.1038/nature13774, 2014.
- 35 Huang, X. J., Liu, Z. R., Zhang, J. K., Wen, T. X., Ji, D. S. and Wang, Y. S.: Seasonal variation and secondary formation of size-segregated aerosol water-soluble inorganic ions during pollution episodes in Beijing, *Atmos. Res.*, 168(September), 70–79, doi:10.1016/j.atmosres.2015.08.021, 2016.



- Ianniello, A., Spataro, F., Esposito, G., Allegrini, I., Hu, M. and Zhu, T.: Chemical characteristics of inorganic ammonium salts in PM_{2.5} in the atmosphere of Beijing (China), *Atmos. Chem. Phys.*, 11(21), 10803–10822, doi:10.5194/acp-11-10803-2011, 2011.
- 5 Karnae, S. and John, K.: Source apportionment of fine particulate matter measured in an industrialized coastal urban area of South Texas, *Atmos. Environ.*, 45(23), 3769–3776, doi:10.1016/j.atmosenv.2011.04.040, 2011.
- Li, J., Du, H. Y., Wang, Z. F., Sun, Y. Le, Yang, W. Y., Li, J. J., Tang, X. and Fu, P. Q.: Rapid formation of a severe regional winter haze episode over a mega-city cluster on the North China Plain, *Environ. Pollut.*, 1–11, doi:10.1016/j.envpol.2017.01.063, 2017.
- 10 Li, L., Chen, Y., Zeng, L., Shao, M., Xie, S., Chen, W., Lu, S., Wu, Y. and Cao, W.: Biomass burning contribution to ambient volatile organic compounds (VOCs) in the chengdu-chongqing region (CCR), China, *Atmos. Environ.*, 99, 403–410, doi:10.1016/j.atmosenv.2014.09.067, 2014.
- Li, P. F., Yan, R. C., Yu, S. C., Wang, S., Liu, W. P. and Bao, H. M.: Reinstatement regional transport of PM_{2.5} as a major cause of severe haze in Beijing, *Proc. Natl. Acad. Sci.*, 112(21), 2–3, doi:10.1073/pnas.1502596112, 2015.
- 15 Li, W. J., Shao, L. Y. and Buseck, P. R.: Haze types in Beijing and the influence of agricultural biomass burning, *Atmos. Chem. Phys.*, 10(17), 8119–8130, doi:10.5194/acp-10-8119-2010, 2010.
- Li, X. R., Wang, L. L., Wang, Y. S., Wen, T. X., Yang, Y. J., Zhao, Y. N. and Wang, Y. F.: Chemical composition and size distribution of airborne particulate matters in Beijing during the 2008 Olympics, *Atmos. Environ.*, 50, 278–286, doi:10.1016/j.atmosenv.2011.12.021, 2012.
- 20 Li, X. R., Song, A. L., Wang, Y. F., Sun, Y., Liu, Z. R. and Wang, Y. S.: Analysis on water-soluble inorganic ions in the atmospheric aerosol of Xinglong, *Environ. Sci.*, 34(1), 15–20(in Chinese), 2013.
- Liang, C. S., Duan, F. K., He, K. B. and Ma, Y. L.: Review on recent progress in observations, source identifications and countermeasures of PM_{2.5}, *Env. Int.*, 86, 150–170, doi:10.1016/j.envint.2015.10.016, 2016.
- 25 Liu, T. T., Gong, S. L., He, J. J., Yu, M., Wang, Q. F., Li, H. R., Liu, W., Zhang, J., Li, L., Wang, X. G., Li, S. L., Lu, Y. L., Du, H. T., Wang, Y. Q., Zhou, C. H., Liu, H. L. and Zhao, Q. C.: Attributions of meteorological and emission factors to the 2015 winter severe haze pollution episodes in China's Jing-Jin-Ji area, *Atmos. Chem. Phys.*, 17, 2971–2980, doi:10.5194/acp-17-2971-2017, 2017.
- 30 Liu, Z. R., Hu, B., Zhang, J. K., Yu, Y. C. and Wang, Y. S.: Characteristics of aerosol size distributions and chemical compositions during wintertime pollution episodes in Beijing, *Atmos. Res.*, 168(August 2015), 1–12, doi:10.1016/j.atmosres.2015.08.013, 2016a.
- Liu, Z. R., Wang, Y. S., Hu, B., Ji, D. S., Zhang, J. K., Wu, F. K., Wan, X. and Wang, Y. H.: Source appointment of fine particle number and volume concentration during severe haze pollution in Beijing in January 2013, *Environ. Sci. Pollut. Res.*, 23(7), 6845–6860, doi:10.1007/s11356-015-5868-6, 2016b.
- 35 Mohiuddin, K., Strezov, V., Nelson, P. F. and Stelcer, E.: Characterisation of trace metals in atmospheric particles in the vicinity of iron and steelmaking industries in Australia, *Atmos. Environ.*, 83(February), 72–79, doi:10.1016/j.atmosenv.2013.11.011, 2014.



- Na, K., Sawant, A. A., Song, C. and Cocker, D. R.: Primary and secondary carbonaceous species in the atmosphere of Western Riverside County, California, *Atmos. Environ.*, 38(9), 1345–1355, doi:10.1016/j.atmosenv.2003.11.023, 2004.
- 5 Peng, J., Hu, M., Du, Z., Wang, Y., Zheng, J., Zhang, W., Yang, Y., Qin, Y., Zheng, R., Xiao, Y., Wu, Y., Lu, S., Wu, Z., Guo, S., Mao, H. and Shuai, S.: Gasoline aromatic: a critical determinant of urban secondary organic aerosol formation, *Atmos. Chem. Phys. Discuss.*, (x), 1–20, doi:10.5194/acp-2017-254, 2017.
- 10 Reff, A., Eberly, S. I. and Bhawe, P. V.: Receptor Modeling of Ambient Particulate Matter Data Using Positive Matrix Factorization: Review of Existing Methods, *J. Air Waste Manag. Assoc.*, 57, 146–154, 2007.
- Saarikoski, S., Timonen, H., Saarnio, K., Aurela, M., Jarvi, M., Keronen, P., Kerminen, V.-M. and Hillamo, R.: Sources of organic carbon in fine particulate matter in northern European urban air, *Atmos. Chem. Phys.*, 8(20), 6281–6295, 2008.
- 15 Schell, B., Ackermann, I. J., Hass, H., Binkowski, F. S. and Ebel, A.: Modeling the formation of secondary organic aerosol within a comprehensive air quality model system, *J. Geophys. Res. Atmos.*, 106(D22), 28275–28293, doi:10.1029/2001JD000384, 2001.
- Shen, R. R., Schäfer, K., Schnelle-Kreis, J., Shao, L. Y., Norra, S., Kramar, U., Michalke, B., Abbaszade, G., Streibel, T., Fricker, M., Chen, Y., Zimmermann, R., Emeis, S. and Schmid, H. P.: Characteristics and sources of PM in seasonal perspective - A case study from one year continuously sampling in Beijing, *Atmos. Pollut. Res.*, 7(2), 235–248, doi:10.1016/j.apr.2015.09.008, 2016.
- 20 Singh, A., Rastogi, N., Patel, A. and Singh, D.: Seasonality in size-segregated ionic composition of ambient particulate pollutants over the Indo-Gangetic Plain: Source apportionment using PMF, *Environ. Pollut.*, 1–10, doi:10.1016/j.envpol.2016.09.010, 2016.
- Sun, Y., Wang, Z., Dong, H., Yang, T., Li, J., Pan, X., Chen, P. and Jayne, J. T.: Characterization of summer organic and inorganic aerosols in Beijing, China with an Aerosol Chemical Speciation Monitor, *Atmos. Environ.*, 51, 250–259, doi:10.1016/j.atmosenv.2012.01.013, 2012.
- 25 Sun, Y. L., Zhuang, G. S., Huang, K., Li, J., Wang, Q. Z., Wang, Y., Lin, Y. F., Fu, J. S., Zhang, W. J., Tang, A. H. and Zhao, X. J.: Asian dust over northern China and its impact on the downstream aerosol chemistry in 2004, *J. Geophys. Res. Atmos.*, 115(11), 1–16, doi:10.1029/2009JD012757, 2010.
- 30 Sun, Y. L., Wang, Z. F., Fu, P. Q., Yang, T., Jiang, Q., Dong, H. B., Li, J. and Jia, J. J.: Aerosol composition, sources and processes during wintertime in Beijing, China, *Atmos. Chem. Phys.*, 13(9), 4577–4592, doi:10.5194/acp-13-4577-2013, 2013.
- Sun, Y. L., Jiang, Q., Xu, Y. S., Ma, Y., Zhang, Y. J., Liu, X. G., Li, W. J., Li, J., Wang, P. C., Wang, F. and Li, Z. Q.: Aerosol characterization over the North China Plain: Haze life cycle and biomass burning impacts in summer, *J. Geophys. Res. Atmos. Res.*, 121, 2508–2521, doi:10.1002/2015JD024261, 2016.
- 35 Tang, G., Zhu, X., Hu, B., Xin, J., Wang, L., Munkel, C., Mao, G. and Wang, Y.: Impact of emission controls on air quality in Beijing during APEC 2014: Lidar ceilometer observations, *Atmos. Chem. Phys.*, 15, 12667–12680, doi:10.5194/acp-15-12667-2015, 2015a.



- Tang, G. Q., Sun, J., Wu, F. K., Sun, Y., Zhu, X. W., Geng, Y. J. and Wang, Y. S.: Organic composition of gasoline and its potential effects on air pollution in North China, *Sci. China Chem.*, 58(9), 1416–1425, doi:10.1007/s11426-015-5464-0, 2015b.
- 5 Tang, G. Q., Zhang, J. Q., Zhu, X. W., Song, T., Münkler, C., Hu, B., Schäfer, K., Liu, Z., Zhang, J. K., Wang, L. L., Xin, J. Y., Suppan, P. and Wang, Y. S.: Mixing layer height and its implications for air pollution over Beijing, China, *Atmos. Chem. Phys.*, 16(4), 2459–2475, doi:10.5194/acp-16-2459-2016, 2016a.
- Tang, G. Q., Chao, N., Wang, Y. S. and Chen, J. S.: Vehicular emissions in China in 2006 and 2010, *J. Environ. Sci. (China)*, 48, 179–192, doi:10.1016/j.jes.2016.01.031, 2016b.
- 10 Tang, G. Q., Zhao, P. S., Wang, Y. H., Gao, W. K., Cheng, M. T., Xin, J. Y., Li, X. and Wang, Y. S.: Mortality and air pollution in Beijing: The long-term relationship, *Atmos. Environ.*, 150, 238–243, doi:10.1016/j.atmosenv.2016.11.045, 2017.
- Tao, J., Zhang, L. M., Cao, J. J., Hsu, S. C., Xia, X. G., Zhang, Z., Lin, Z. J., Cheng, T. T. and Zhang, R. J.: Characterization and source apportionment of aerosol light extinction in Chengdu, southwest
15 China, *Atmos. Environ.*, 95, 552–562, doi:10.1016/j.atmosenv.2014.07.017, 2014.
- Tao, M. H., Chen, L. F., Su, L. and Tao, J. H.: Satellite observation of regional haze pollution over the North China Plain, *J. Geophys. Res. Atmos.*, 117, D12203, doi:10.1029/2012JD017915, 2012.
- Tian, S. L., Pan, Y. P. and Wang, Y. S.: Size-resolved source apportionment of particulate matter in urban Beijing during haze and non-haze episodes, *Atmos. Chem. Phys.*, 16(1), 1–19,
20 doi:10.5194/acp-16-1-2016, 2016.
- Turpin, B. J. and Lim, H.: Species Contributions to PM_{2.5} Mass Concentrations: Revisiting Common Assumptions for Estimating Organic Mass, *Aerosol Sci. Technol.*, 35(1), 602–610, doi:10.1080/02786820119445, 2001.
- 25 U.S. Environmental Protection Agency: EPA Positive Matrix Factorization (PMF) 5.0 Fundamentals and User Guide, 2014.
- Wang, G., Cheng, S. Y., Li, J. B., Lang, J. L., Wen, W., Yang, X. W. and Tian, L.: Source apportionment and seasonal variation of PM_{2.5} carbonaceous aerosol in the Beijing-Tianjin-Hebei region of China, *Env. Monit Assess.*, 187(3), 143, doi:10.1007/s10661-015-4288-x, 2015a.
- 30 Wang, G., Zhang, R., Gomez, M. E., Yang, L., Levy Zamora, M., Hu, M., Lin, Y., Peng, J., Guo, S., Meng, J., Li, J., Cheng, C., Hu, T., Ren, Y., Wang, Y., Gao, J., Cao, J., An, Z., Zhou, W., Li, G., Wang, J., Tian, P., Marrero-Ortiz, W., Secrest, J., Du, Z., Zheng, J., Shang, D., Zeng, L., Shao, M., Wang, W., Huang, Y., Wang, Y., Zhu, Y., Li, Y., Hu, J., Pan, B., Cai, L., Cheng, Y., Ji, Y., Zhang, F., Rosenfeld, D., Liss, P. S., Duce, R. A., Kolb, C. E. and Molina, M. J.: Persistent sulfate formation from London Fog to Chinese haze., *Proc. Natl. Acad. Sci. U. S. A.*, 113(48), 13630–13635,
35 doi:10.1073/pnas.1616540113, 2016a.
- Wang, G. H., Zhou, B. H., Cheng, C. L., Cao, J. J., Li, J. J., Meng, J. J., Tao, J., Zhang, R. J. and Fu, P. Q.: Impact of Gobi desert dust on aerosol chemistry of Xi'an, inland China during spring 2009: differences in composition and size distribution between the urban ground surface and the mountain atmosphere, *Atmos. Chem. Phys.*, 13(2), 819–835, doi:10.5194/acp-13-819-2013, 2013a.



- Wang, J., Pan, Y. P., Tian, S. L., Chen, X., Wang, L. and Wang, Y. S.: Size distributions and health risks of particulate trace elements in rural areas in northeastern China, *Atmos. Res.*, 168, 191–204, doi:10.1016/j.atmosres.2015.08.019, 2016b.
- 5 Wang, L. T., Xu, J., Yang, J., Zhao, X. J., Wei, W., Cheng, D. D., Pan, X. M. and Su, J.: Understanding haze pollution over the southern Hebei area of China using the CMAQ model, *Atmos. Environ.*, 56, 69–79, doi:10.1016/j.atmosenv.2012.04.013, 2012a.
- Wang, L. T., Wei, Z., Yang, J., Zhang, Y., Zhang, F. F., Su, J., Meng, C. C. and Zhang, Q.: The 2013 severe haze over southern Hebei, China: Model evaluation, source apportionment, and policy implications, *Atmos. Chem. Phys.*, 14(6), 3151–3173, doi:10.5194/acp-14-3151-2014, 2014a.
- 10 Wang, X. F., Wang, W. X., Yang, L. X., Gao, X. M., Nie, W., Yu, Y. C., Xu, P. J., Zhou, Y. and Wang, Z.: The secondary formation of inorganic aerosols in the droplet mode through heterogeneous aqueous reactions under haze conditions, *Atmos. Environ.*, 63, 68–76, doi:10.1016/j.atmosenv.2012.09.029, 2012b.
- Wang, Y., Yao, L., Wang, L., Liu, Z., Ji, D., Tang, G., Zhang, J., Sun, Y., Hu, B. and Xin, J.:
15 Mechanism for the formation of the January 2013 heavy haze pollution episode over central and eastern China, *Sci. China Earth Sci.*, 57(1), 14–25, doi:10.1007/s11430-013-4773-4, 2013b.
- Wang, Y. H., Liu, Z. R., Zhang, J. K., Hu, B., Ji, D. S., Yu, Y. C. and Wang, Y. S.: Aerosol physicochemical properties and implications for visibility during an intense haze episode during winter in Beijing, *Atmos. Chem. Phys.*, 15(6), 3205–3215, doi:10.5194/acp-15-3205-2015, 2015b.
- 20 Wang, Y. S., Yao, L., Wang, L. L., Liu, Z. R., Ji, D. S., Tang, G. Q., Zhang, J. K., Sun, Y., Hu, B. and Xin, J. Y.: Mechanism for the formation of the January 2013 heavy haze pollution episode over central and eastern China, *Sci. China Earth Sci.*, 57(1), 14–25, doi:10.1007/s11430-013-4773-4, 2014b.
- Watson, J. G., Chow, J. C. and Houck, J. E.: PM_{2.5} chemical source profiles for vehicle exhaust, vegetative burning, geological material, and coal burning in Northwestern Colorado during 1995,
25 *Chemosphere*, 43(8), 1141–1151, doi:10.1016/S0045-6535(00)00171-5, 2001.
- Wu, D., Mao, J. T., Deng, X. J., Tie, X. X., Zhang, Y. H., Zeng, L. M., Li, F., Tan, H. B., Bi, X. Y., Huang, X. Y., Chen, J. and Deng, T.: Black carbon aerosols and their radiative properties in the Pearl River Delta region, *Sci. China, Ser. D Earth Sci.*, 52(8), 1152–1163, doi:10.1007/s11430-009-0115-y, 2009.
- 30 Wu, R., Dai, H. C., Geng, Y., Xie, Y., Masui, T., Liu, Z. Q. and Qian, Y. Y.: Economic Impacts from PM_{2.5} Pollution-Related Health Effects: A Case Study in Shanghai, *Environ. Sci. Technol.*, acs.est.7b00026, doi:10.1021/acs.est.7b00026, 2017.
- Xu, W. Y., Zhao, C. S., Ran, L., Deng, Z. Z., Liu, P. F., Ma, N., Lin, W. L., Xu, X. B., Yan, P., He, X., Yu, J., Liang, W. D. and Chen, L. L.: Characteristics of pollutants and their correlation to
35 meteorological conditions at a suburban site in the North China Plain, *Atmos. Chem. Phys.*, 11(9), 4353–4369, doi:10.5194/acp-11-4353-2011, 2011.
- Yang, L. X., Zhou, X. H., Wang, Z., Zhou, Y., Cheng, S. H., Xu, P. J., Gao, X. M., Nie, W., Wang, X. F. and Wang, W. X.: Airborne fine particulate pollution in Jinan, China: Concentrations, chemical compositions and influence on visibility impairment, *Atmos. Environ.*, 55, 506–514,



- doi:10.1016/j.atmosenv.2012.02.029, 2012.
- Ying, Q., Wu, L. and Zhang, H. L.: Local and inter-regional contributions to PM_{2.5} nitrate and sulfate in China, *Atmos. Environ.*, 94, 582–592, doi:10.1016/j.atmosenv.2014.05.078, 2014.
- Yuan, B., Liu, Y., Shao, M., Lu, S. H. and Streets, D. G.: Biomass burning contributions to ambient VOCs species at a receptor site in the Pearl River delta (PRD), China, *Environ. Sci. Technol.*, 44(12), 4577–4582, doi:10.1021/es1003389, 2010.
- Zhang, J. K., Sun, Y., Liu, Z. R., Ji, D. S., Hu, B., Liu, Q. and Wang, Y. S.: Characterization of submicron aerosols during a month of serious pollution in Beijing, 2013., *Atmos. Chem. Phys.*, 14, 2887–2903, doi:10.5194/acp-14-2887-2014, 2014.
- 10 Zhang, J. K., Wang, Y. S., Huang, X. J., Liu, Z. R., Ji, D. S. and Sun, Y.: Characterization of Organic Aerosols in Beijing Using an Aerodyne High-Resolution Aerosol Mass Spectrometer, *Adv. Atmos. Sci.*, 32, 877–888, doi:10.1007/s00376-014-4153-9, 2015a.
- Zhang, K., Batterman, S. and Dion, F.: Vehicle emissions in congestion: Comparison of work zone, rush hour and free-flow conditions, *Atmos. Environ.*, 45(11), 1929–1939, doi:10.1016/j.atmosenv.2011.01.030, 2011.
- 15 Zhang, R., Jing, J., Tao, J., Hsu, S. C., Wang, G., Cao, J., Lee, C. S. L., Zhu, L., Chen, Z., Zhao, Y. and Shen, Z.: Chemical characterization and source apportionment of PM_{2.5} in Beijing: seasonal perspective, *Atmos. Chem. Phys.*, 13(14), 7053–7074, doi:10.5194/acp-13-7053-2013, 2013.
- Zhang, R. Y., Wang, G. H., Guo, S., Zamora, M. L., Ying, Q., Lin, Y., Wang, W. gang, Hu, M. and Wang, Y.: Formation of urban fine particulate matter, *Chem Rev*, 115(10), 3803–3855, doi:10.1021/acs.chemrev.5b00067, 2015b.
- 20 Zhang, X. Y., Wang, Y. Q., Niu, T., Zhang, X. C., Gong, S. L., Zhang, Y. M. and Sun, J. Y.: Atmospheric aerosol compositions in China: spatial/temporal variability, chemical signature, regional haze distribution and comparisons with global aerosols, *Atmos. Chem. Phys.*, 12(2), 779–799, doi:10.5194/acp-12-779-2012, 2012.
- 25 Zhang, Y. J., Zheng, M., Cai, J., Yan, C. Q., Hu, Y. T., Russell, A. G., Wang, X. S., Wang, S. X. and Zhang, Y. H.: Comparison and overview of PM_{2.5} source apportionment methods, *Chinese Sci. Bull. (Chinese Version)*, 60(2), 109–121, doi:10.1360/n972014-00975, 2015c.
- Zhang, Y. L. and Cao, F.: Fine particulate matter (PM_{2.5}) in China at a city level, *Sci Rep*, 5, 14884, doi:10.1038/srep14884, 2015.
- 30 Zhao, B., Wang, P., Ma, J. Z., Zhu, S., Pozzer, A. and Li, W.: A high-resolution emission inventory of primary pollutants for the Huabei region, China, *Atmos. Chem. Phys.*, 12(1), 481–501, doi:10.5194/acp-12-481-2012, 2012.
- Zhao, P. S., Dong, F., Yang, Y. D., He, D., Zhao, X. J., Zhang, W. Z., Yao, Q. and Liu, H. Y.: Characteristics of carbonaceous aerosol in the region of Beijing, Tianjin, and Hebei, China, *Atmos. Environ.*, 71, 389–398, doi:10.1016/j.atmosenv.2013.02.010, 2013a.
- 35 Zhao, P. S., Dong, F., He, D., Zhao, X. J., Zhang, X. L., Zhang, W. Z., Yao, Q. and Liu, H. Y.: Characteristics of concentrations and chemical compositions for PM_{2.5} in the region of Beijing,



- Tianjin, and Hebei, China, Atmos. Chem. Phys., 13(9), 4631–4644, doi:10.5194/acp-13-4631-2013, 2013b.
- Zhao, X. J., Zhang, X. L., Xu, X. F., Xu, J., Meng, W. and Pu, W. W.: Seasonal and diurnal variations of ambient PM_{2.5} concentration in urban and rural environments in Beijing, Atmos. Environ., 43(18), 2893–2900, doi:10.1016/j.atmosenv.2009.03.009, 2009.
- Zhao, X. J., Zhao, P. S., Xu, J., Meng, W., Pu, W. W., Dong, F., He, D. and Shi, Q. F.: Analysis of a winter regional haze event and its formation mechanism in the North China Plain, Atmos. Chem. Phys., 13(11), 5685–5696, doi:10.5194/acp-13-5685-2013, 2013c.
- Zhu, X., Tang, G., Hu, B., Wang, L., Xin, J., Zhang, J., Liu, Z., Münkler, C. and Wang, Y.: Regional pollution and its formation mechanism over North China Plain: A case study with ceilometer observations and model simulations, J. Geophys. Res. Atmos., 1–15, doi:10.1002/2016JD025730, 2016.
- Zong, Z., Wang, X. P., Tian, C. G., Chen, Y. J., Qu, L., Ji, L., Zhi, G. R., Li, J. and Zhang, G.: Source apportionment of PM_{2.5} at a regional background site in North China using PMF linked with radiocarbon analysis: Insight into the contribution of biomass burning, Atmos. Chem. Phys., 16(17), 11249–11265, doi:10.5194/acp-16-11249-2016, 2016.